

See discussions, stats, and author profiles for this publication at: <https://www.researchgate.net/publication/273700264>

# Aryl Hydrocarbon Receptor Ligand 5F 203 Induces Oxidative Stress That Triggers DNA Damage in Human Breast Cancer Cells

ARTICLE in CHEMICAL RESEARCH IN TOXICOLOGY · MARCH 2015

Impact Factor: 3.53 · DOI: 10.1021/tx500485v · Source: PubMed

CITATIONS

2

READS

50

14 AUTHORS, INCLUDING:



[Lancelot Mclean](#)

Loma Linda University

9 PUBLICATIONS 55 CITATIONS

[SEE PROFILE](#)



[Willie L Davis](#)

Loma Linda University

5 PUBLICATIONS 22 CITATIONS

[SEE PROFILE](#)



[Lawrence C Sowers](#)

Loma Linda University

53 PUBLICATIONS 1,917 CITATIONS

[SEE PROFILE](#)



[Eileen Brantley](#)

Loma Linda University

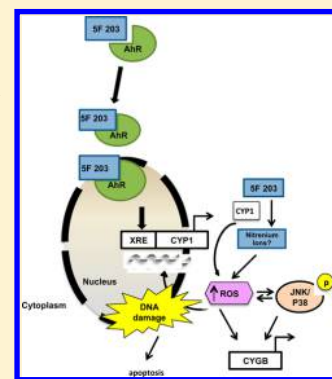
15 PUBLICATIONS 187 CITATIONS

[SEE PROFILE](#)

## Aryl Hydrocarbon Receptor Ligand 5F 203 Induces Oxidative Stress That Triggers DNA Damage in Human Breast Cancer Cells

Lancelot S. McLean,<sup>†</sup> Cheri N. Watkins,<sup>‡</sup> Petreena Campbell,<sup>‡</sup> Dain Zylstra,<sup>§</sup> Leah Rowland,<sup>‡</sup> Louisa H. Amis,<sup>‡</sup> Lia Scott,<sup>‡</sup> Crystal E. Babb,<sup>‡</sup> W. Joel Livingston,<sup>‡</sup> Agus Darwanto,<sup>‡,¶</sup> Willie L. Davis, Jr.,<sup>‡,§</sup> Maheswari Senthil,<sup>||</sup> Lawrence C. Sowers,<sup>⊥</sup> and Eileen Brantley<sup>\*,‡,§</sup><sup>†</sup>Center for Dental Research, School of Dentistry, <sup>‡</sup>Department of Basic Sciences, School of Medicine, <sup>§</sup>Department of Pharmaceutical and Administrative Sciences, School of Pharmacy, <sup>||</sup>Department of Surgery, School of Medicine, Loma Linda University Health, Loma Linda, California 92350, United States<sup>⊥</sup>Department of Pharmacology and Toxicology, University of Texas Medical Branch at Galveston, Galveston, Texas 77555, United States

**ABSTRACT:** Breast tumors often show profound sensitivity to exogenous oxidative stress. Investigational agent 2-(4-amino-3-methylphenyl)-5-fluorobenzothiazole (5F 203) induces aryl hydrocarbon receptor (AhR)-mediated DNA damage in certain breast cancer cells. Since AhR agonists often elevate intracellular oxidative stress, we hypothesize that 5F 203 increases reactive oxygen species (ROS) to induce DNA damage, which thwarts breast cancer cell growth. We found that 5F 203 induced single-strand break formation. 5F 203 enhanced oxidative DNA damage that was specific to breast cancer cells sensitive to its cytotoxic actions, as it did not increase oxidative DNA damage or ROS formation in nontumorigenic MCF-10A breast epithelial cells. In contrast, AhR agonist and procarcinogen benzo[*a*]pyrene and its metabolite, 1,6-benzo[*a*]pyrene quinone, induced oxidative DNA damage and ROS formation, respectively, in MCF-10A cells. In sensitive breast cancer cells, 5F 203 activated ROS-responsive kinases: c-Jun-N-terminal kinase (JNK) and p38 mitogen activated protein kinase (p38). AhR antagonists (alpha-naphthoflavone, CH223191) or antioxidants (*N*-acetyl-L-cysteine, EUK-134) attenuated 5F 203-mediated JNK and p38 activation, depending on the cell type. Pharmacological inhibition of AhR, JNK, or p38 attenuated 5F 203-mediated increases in intracellular ROS, apoptosis, and single-strand break formation. 5F 203 induced the expression of cytoglobin, an oxidative stress-responsive gene and a putative tumor suppressor, which was diminished with AhR, JNK, or p38 inhibition. Additionally, 5F 203-mediated increases in ROS production and cytoglobin were suppressed in AHR100 cells (AhR ligand-unresponsive MCF-7 breast cancer cells). Our data demonstrate 5F 203 induces ROS-mediated DNA damage at least in part via AhR, JNK, or p38 activation and modulates the expression of oxidative stress-responsive genes such as cytoglobin to confer its anticancer action.



## 1. INTRODUCTION

Breast cancer is the most common form of cancer among women and kills nearly 40 000 women each year in the US.<sup>1–3</sup> Breast cancer cells often contain excessive reactive oxygen species (ROS) levels in comparison to that in nonmalignant breast epithelial cells. In particular, breast cancer cells with low estrogen receptor alpha relative to estrogen receptor beta protein expression levels contain elevated levels of ROS.<sup>4</sup> These basally elevated levels of ROS can be exploited pharmacologically by further increasing oxidative stress within these cells to trigger cytotoxicity and DNA damage. Such a therapeutic strategy is promising since nonmalignant tissues show less susceptibility to drug-mediated increases in ROS levels when compared to that in malignant tissues.

The investigational agent 2-(4-amino-3-methylphenyl)-5-fluorobenzothiazole (5F 203) displays selective and potent anticancer activity *in vitro*, and its prodrug lysylamide derivative (Phortress) retains this selectivity and potency profile *in vivo*.<sup>5–7</sup> 5F 203 is an AhR agonist<sup>8</sup> that activates the AhR signaling pathway and causes DNA damage, cell cycle arrest,

and apoptosis in breast cancer cells that are sensitive to its cytotoxic actions.<sup>9–12</sup> Similar to the mechanism of other AhR agonists, 5F 203 binds to AhR, and the 5F 203–AhR complex translocates from the cytosol to the nucleus. Once within the nucleus, the 5F 203–AhR complex binds to xenobiotic response elements within the respective promoters of target genes, such as *cytochrome P450 1A1* (CYP1A1), to activate their transcription. 5F 203-mediated CYP1A1 induction promotes its bioconversion into metabolites that presumably exhibit anticancer activity.<sup>11</sup>

We and others have shown that AhR agonists increase ROS levels in breast cancer cells.<sup>13–15</sup> Increased intracellular ROS formation frequently leads to activation of mitogen activated protein kinases (MAPKs) such as c-Jun-amino-terminal kinase (JNK), extracellular signal regulated kinase (ERK), and p38 mitogen activated protein kinase (p38).<sup>16,17</sup> MAPKs regulate a number of physiological processes including apoptosis, angio-

Received: November 25, 2014

genesis, and cell motility.<sup>18–20</sup> Stress stimuli, such as increased ROS, promote Ras binding to an upstream MAPK family member, thus triggering a cascade of events that culminate in the phosphorylation of several tiers of kinases critical to eliciting distinct cellular responses.<sup>21,22</sup> In breast cells, ROS-induced cellular stress has been demonstrated to activate JNK and p38, thereby promoting both breast epithelial cell differentiation and breast cancer cell death.<sup>23,24</sup> While ERK signaling tends to promote cell migration and metastasis, along with cell survival mechanisms,<sup>25</sup> more recent reports have also shown that this kinase can mediate breast cancer cell death.<sup>26–28</sup>

Anticancer agents frequently activate JNK and p38 pathways as part of their mechanism of action, and there are reports that describe p38- and JNK-dependent drug-induced DNA damage.<sup>1,21</sup> Notably, there have been additional reports of cross-talk between the ROS-responsive JNK and p38 pathways and AhR signaling pathways.<sup>29,30</sup> JNK and p38 signaling pathways often regulate genes, including tumor suppressor genes, that prevent the development of a malignant phenotype.<sup>31–34</sup>

SF 203 has been shown to increase ROS production, activate MAPKs, and promote CYP1A1-dependent DNA damage in sensitive ovarian cancer cells.<sup>12</sup> Though SF 203 has been previously shown to induce DNA damage in certain breast cancer cells,<sup>6,11,12,35</sup> to the best of our knowledge, our study is the first to identify specific oxidative stress-related genes whose expression is altered by SF 203. The present study was designed to test the hypothesis that SF 203 increases intracellular ROS and MAPKs to induce DNA damage and the expression of oxidative stress responsive genes as part of its mechanism of action in breast cancer cells. To test this hypothesis, we evaluated ROS levels and DNA damage in a panel of sensitive and insensitive human breast cell lines using flow cytometry-based methods and the comet assay after these cells were exposed to SF 203. Using pharmacological inhibitors, we also evaluated the contribution of JNK and p38 to SF 203-mediated DNA damage in select human breast cell lines. Finally, using PCR array, we examined the ability of SF 203 to modulate a profile of oxidative stress responsive-genes, including putative tumor suppressor gene *cytoglobin* (CYGB), in select breast cancer cells.

## 2. MATERIALS AND METHODS

**Caution:** These chemicals are dangerous. BAP is an established procarcinogen and as such should be handled with proper protection in accordance with the MSDS, which includes the use of lab coat, safety glasses, and gloves. Although 1,6-BPQ is not an established carcinogen, it is recommended that care be used in handling this chemical because it is a metabolite of BAP, a known procarcinogen. This will entail the use of a lab coat, gloves, and safety glasses.

**2.1. Cell Culture and Reagents.** MDA-MB-468, CRL2335, and MCF-7 human breast cancer cell lines, along with MCF-10A human breast epithelial cell line, were obtained from the American Type Culture Collection (ATCC). MDA-MB-231 and T47D human breast cancer cells were obtained from the Frederick National Laboratory for Cancer Research, Division of Cancer Treatment and Diagnosis Tumor Repository. Transformed, AhR ligand-unresponsive MCF-7 human breast cancer cells (AHR100 cells) were a kind gift from Dr. Jason Matthews (University of Toronto, Toronto, CA). A description of the characterization and use of AHR100 cells has been previously described.<sup>36,37</sup> The culture conditions for each cell line have been detailed in a previous report.<sup>14</sup> 2-(4-Amino-3-methylphenyl)-5-fluorobenzothiazole (SF 203, NSC 703786) was obtained from the NCI/DTP Open Chemical Repository (<http://dtp.cancer.gov>, Fred-

erick, MD) at the Frederick National Laboratory for Cancer Research. Stock solutions of SF 203 (10 mM), doxorubicin, (Dox, 1 mM), 5-aza-2'-deoxycytidine (5-Aza, 1 mM), BAP, benzo[a]pyrene-1,6 quinone (1,6-BPQ, 1 mM), alpha-naphthoflavone ( $\alpha$ NF, 1 mM, AhR inhibitor), CH223191 (10 mM, AhR inhibitor), SB202190 (p38 inhibitor, 25 mM), SP600125 (JNK inhibitor, 25 mM), CC-401 (JNK inhibitor, Abcam, 10 mM), Actinomycin D (Act. D, 1mM), and EUK134 (100 mM, superoxide dismutase/catalase mimetic and antioxidant) were dissolved in dimethyl sulfoxide (DMSO) and stored protected from light at  $-20^{\circ}\text{C}$  until use. SB202190 is a highly selective p38 inhibitor.<sup>38</sup> The antioxidant N-acetyl-L-cysteine (NAC) was made up fresh, dissolving it in medium just before use in experiments. Immediately before use, the stock solutions were diluted in complete medium to the desired final concentrations. Alamar Blue dye was purchased from BioSource International, Inc. (Camarillo, CA). The OxyDNA Assay fluorometric kit was purchased from Calbiochem (San Diego, CA). The BAP metabolite 1,6-BPQ was obtained from the NCI Chemical Carcinogen Reference Standards Repository Midwest Research Institute (Kansas City, MO). ERK1/2, phospho-ERK 1/2, JNK1/2, p38, and phospho-p38 antibodies were purchased from Cell Signaling Technology (Danvers, MA). Antibodies for phospho-JNK were obtained from Cell Signaling Technology (Danvers, MA) or Santa Cruz Biotechnology (Santa Cruz, CA). Antibodies for GAPDH and beta actin were obtained from Santa Cruz Biotechnology (Santa Cruz, CA) or from Sigma-Aldrich (St. Louis, MO), respectively. All other reagents were purchased from Sigma-Aldrich (St. Louis, MO).

**2.2. Alamar Blue Assay.** We evaluated SF 203-mediated cytotoxicity using the Alamar Blue assay in a breast cell line panel as previously described.<sup>14</sup> Briefly, cells were plated in 96-well plates at their appropriate densities in a total volume of 200  $\mu\text{L}$ . After 24 h of incubation, cells were treated with medium containing 0.1% DMSO or varying concentrations of SF 203 for 72 h before 20  $\mu\text{L}$  of Alamar Blue dye was added to fresh medium followed by an additional 4–5 h incubation. In some studies, MDA-MB-468 breast cancer cells were exposed to SF 203 at varying concentrations for 12–48 h. SF 203-mediated cytotoxicity was determined using an FLx800 microplate spectrofluorometer (BioTek Instruments, USA) set with excitation at 530 nm and emission at 590 nm.

**2.3. Relief Contrast Microscopy.** Apoptosis was assessed qualitatively using an Olympus IX71 inverted microscope equipped with relief contrast and SPOT imaging as previously described.<sup>14</sup> Briefly, MDA-MB-468 cells were treated for 12 h with 0.1% DMSO, 100 nM  $\alpha$ NF, 25  $\mu\text{M}$  SP60125, 25  $\mu\text{M}$  SB202190, or 1.0  $\mu\text{M}$  SF 203 with or without a 1 h  $\alpha$ NF, JNK SP600125, or SB202190 pretreatment. Following treatment, cells were visualized microscopically to detect apoptotic body formation.

**2.4. Measurement of Intracellular Reactive Oxygen Species.** Intracellular ROS levels were measured in breast cancer cells or MCF-10A breast epithelial cells after exposure to SF 203 as described previously.<sup>14</sup> Briefly, cells were exposed to medium containing 0.1% DMSO or 1  $\mu\text{M}$  SF 203 for specified time intervals prior to staining with 2',7'-dichlorodihydrofluorescein diacetate ( $\text{H}_2\text{DCF-DA}$ ) for 30 min at  $37^{\circ}\text{C}$ . Cells were harvested and analyzed by a FACScan flow cytometer (Becton Dickinson, Franklin Lakes, NJ). In some experiments, cells were exposed to antioxidants (NAC or EUK134), JNK inhibitors (SP600125 or CC-401), SB202190, or  $\alpha$ NF for 6 h alone or for 1 h prior to cotreatment with SF 203. In other experiments, cells were pretreated for 30 min with SP600125 or SB202190 prior to shorter (1 or 3 h) SF 203 treatments before determining intracellular ROS levels using flow cytometry.

Alternatively, MCF-10A cells were exposed to medium containing either 0.1% DMSO, 1  $\mu\text{M}$  SF 203, or 2  $\mu\text{M}$  1,6-BPQ for 2 h, and ROS was determined in accordance with a previously described method.<sup>40</sup> In brief, cells were exposed to 10  $\mu\text{M}$   $\text{H}_2\text{DCF-DA}$  dye for 15 min. The medium was then removed and replaced with the treatments mentioned above, and the cells were analyzed by flow cytometry.

**2.5. Comet Assay.** MDA-MB-468 cells were seeded into 25  $\text{cm}^2$  tissue culture flasks at a density of  $5.0 \times 10^5$  cells/flask. After 24 h, cells were treated for 12 h with either 0.1% DMSO, doxorubicin, varying



concentrations of SF 203, SP600125, SB202190,  $\alpha$ NF, or SF 203 with or without 1 h pretreatment of SP600125, SB202190, or  $\alpha$ NF. After treatment, cells were harvested with trypsin and processed in ice-cold PBS at a final density of  $1.0 \times 10^5$  cells/mL, according to the manufacturer's instructions. Aliquots were taken from each cell sample and added to low-melting agarose gel at 40 °C in a 1:10 v/v suspension. The agarose suspension was loaded onto Trevigen CometSlides (Gaithersburg, MD) and allowed to harden (20 min, 4 °C). All of the steps above were performed in dim light to minimize DNA damage artifacts.

The CometSlides were placed in prechilled comet lysis buffer for 1 h at 4 °C. Slides were transferred into an alkaline buffer [200 mM NaOH, 1 mM EDTA (pH > 13)] for 20 min in the dark to unwind the DNA and convert alkali-labile sites to single-strand breaks (SSBs). Following the unwinding step, slides were subjected to electrophoresis using the same alkaline buffer (stored at 4 °C) for 30 min at 21 V (1 V/cm). After electrophoresis, slides were washed twice with deionized H<sub>2</sub>O for 10 min each and dehydrated in ethanol for 5 min. DNA fragments created by SSBs migrate much faster than undamaged DNA when subjected to an electric field, resulting in the moment of cleaved DNA, or the comet tail. Undamaged DNA remains within the cell nucleoid.

After drying completely, slides were stained with SYBR Gold nucleic acid gel stain (diluted 1:50000 in TE buffer), which has superior sensitivity for detecting single- and double-stranded DNA. At least 90 cells were randomly selected from each sample and analyzed using a fluorescence microscope and the Comet Assay IV software scoring system (Perceptive Instruments, UK) to quantify DNA damage in individual cells. DNA damage as described by SSB formation is reported as percent tail intensity, which compares the relative intensity of genetic material in the comet tail to the intensity of the genetic material in the comet head.

**2.6. DNA Isolation and Oxidative DNA Damage Analysis.** MDA-MB-468 cells were treated for 12 h with either 0.1% DMSO (control) or 1  $\mu$ M SF 203. Cells treated with 100  $\mu$ M buthionine sulfoximine (BSO) for 18 h followed by 500  $\mu$ M H<sub>2</sub>O<sub>2</sub> for 30 min served as a positive control for these experiments. DNA isolation was performed as previously described.<sup>41</sup> Extracted DNA was hydrolyzed, and 8-hydroxy-2'-deoxyguanosine (8-oxodG) levels were measured using HPLC with electrochemical detection (HPLC-ECD) as previously reported.<sup>14</sup> Adventitious oxidation of dGuo was prevented by the use of the metal ion chelator deferoxamine mesylate (DFAM).

Alternatively, oxidative DNA damage in MDA-MB-468 cells was evaluated using a fluorometric OxyDNA assay (EMD4 Biosciences, Darmstadt, Germany) as previously reported.<sup>42</sup> This assay detects the 8-oxoguanine lesion using a FITC-labeled binding protein conjugate linked to an antigenic determinant on 8-oxoguanine of oxidized DNA. In brief, cells were treated as described for those analyzed via the HPLC-ECD method before cells were harvested, fixed, permeabilized, washed, resuspended in PBS, and stained, followed by analysis using the OxyDNA assay. To avoid quenching superoxide radicals, the total DMSO percentage did not exceed 0.02% in any of the treatments for the OxyDNA assay, unlike that in the HPLC-ECD method. Alternatively, MCF-10A cells were exposed to medium containing either 0.02% DMSO, 1  $\mu$ M SF 203, or varying concentrations of BAP before analysis with the OxyDNA assay.

**2.7. Immunoblotting for Detecting MAPK Phosphorylation.** MDA-MB-468 and T47D cells were seeded at  $(1-3) \times 10^6$  per plate (100 mm) 24 h before being incubated in serum-free medium for an additional 24 h. The cells were then treated with medium containing 1  $\mu$ M SF 203 or 0.1% DMSO for 0–12 h. In some cases, MDA-MB-468 cells received antioxidant, AHR inhibitor, SB202190, or JNK inhibitor 1 h pretreatment prior to SF 203 treatment for 6 h. Following treatment, the cells were harvested and washed with cold PBS before adding cold lysis buffer (100 mM Tris-HCl [pH 6.8], 4% SDS, 10% glycerol [v/v], and complete protease inhibitor cocktail) for 30 min at 4 °C. Protein concentration was determined using the D<sub>C</sub> protein assay kit according to the manufacturer's instructions (Bio-Rad, Hercules, CA). Proteins were resolved on 4–12% SDS-polyacrylamide gel and transferred via electrophoresis onto nitrocellulose or poly(vinyl difluoride) mem-

branes. The membranes were blocked with blocking buffer consisting of 5% nonfat dry milk in 1% Tween 20 in 20 mM TBS (pH 7.5) for 1 h at room temperature. Afterward, the membranes were incubated overnight at 4 °C in 5% BSA-based buffer with rabbit primary antibodies against phosphorylated forms of ERK and p38 and total forms of ERK, JNK, or p38 (1:1000 dilution). In certain cases, when using antibodies for phosphorylated JNK, membranes were blocked overnight at 4 °C and incubated in mouse primary antibody (1:100 dilution or 1:500 dilution) from Santa Cruz Biotechnology (Santa Cruz, CA) for 1 h. Membranes were then incubated with the appropriate HRP-conjugated secondary antibodies (Cell Signaling Technology, Danvers MA or Santa Cruz Biotechnology, Santa Cruz, CA) for 1 h at the appropriate dilution at room temperature and visualized using a standard enhanced chemiluminescence detection system or the Super Signal West Dura chemiluminescent substrate (Thermo Scientific, Barrington, IL).

**2.8. Glutathione Assay.** MDA-MB-468 cells were plated in 25 cm<sup>2</sup> flasks at  $1 \times 10^6$  cells/flask and cultured overnight in the presence of 5% CO<sub>2</sub> at 37 °C. Cells in triplicate were treated 24 h later with 1  $\mu$ M SF 203 or 0.1% DMSO for 12 h to induce apoptosis. At the end of the time point, intracellular GSH levels were measured using the monochlorobimane (MCB) glutathione detection assay according to the manufacturer's instructions. Fluorescence was measured (excitation at 395 nm and emission at 480 nm) using an FLx800 microplate fluorescence reader.

**2.9. RNA Extraction.** Total RNA was isolated from CRL-2335, MCF-7, T47D, MDA-MB-231, and MDA-MB-468 breast cancer cells following the appropriate treatments using the Aurum total RNA mini kit (Bio-Rad, Hercules, CA). The quantity of RNA in the extracts was determined by measuring the absorbance at 260 and 280 nm using a Beckman DU 800 spectrophotometer (Beckman, Brea, CA). RNA quality was further analyzed, and RNA quality indicator (RQI) values were determined using the Experion automated electrophoresis system (Bio-Rad, Hercules, CA).

**2.10. Human Oxidative Stress and Antioxidant Defense PCR Array.** Complementary DNA (cDNA) was prepared from 1  $\mu$ g aliquots of total RNA samples from CRL 2335, MCF-7, and MDA-MB-468 breast cancer cells using the RT<sup>2</sup> first strand synthesis kit (SA Biosciences, Frederick, MD). Briefly, each sample was mixed with 2  $\mu$ L of 5 $\times$  genomic DNA elimination buffer to make up a final volume of 10  $\mu$ L, incubated at 42 °C for 5 min, and chilled on ice for at least 1 min. RT cocktail (10  $\mu$ L), prepared according to the manufacturer's instructions, was added to 10  $\mu$ L of genomic DNA elimination mixture and incubated at 42 °C for 15 min, followed by heating at 95 °C for 5 min. ddH<sub>2</sub>O (91  $\mu$ L) was added to each 20  $\mu$ L of cDNA synthesis reaction. Real-time PCR was performed using the human oxidative stress and antioxidant defense RT<sup>2</sup> profiler PCR array according to the manufacturer's instructions (SA Biosciences, Frederick, MD). Gene expression analysis was performed using the web-based RT<sup>2</sup> profiler PCR array data analysis program (SA Biosciences, Frederick, MD). Relative gene expression was determined using  $\Delta\Delta C_T$ -based fold-change values calculated from the experimental  $C_T$  values after normalization to the averaged means of five housekeeping genes housekeeping genes. The housekeeping genes used were beta 2-microglobulin (B2M), hypoxanthine phosphoribosyltransferase I (HPRT1), 60S ribosomal protein L13a (RPL13A), glyceraldehyde 3-phosphate dehydrogenase (GAPDH), and beta actin (ACTB).

**2.11. Real-Time Quantitative RT-PCR Analysis.** RNA was extracted from select breast cancer cells following specified treatments using the iScript cDNA synthesis kit (Bio-Rad, Hercules, CA) according to the manufacturer's instructions. The cDNA was used as a template for real-time quantitative PCR analysis using a CFX-96 PCR instrument (Bio-Rad, Hercules, CA). The primers for the GAPDH and cytoglobin (CYGB) genes were obtained from SA Biosciences (Frederick, MD). The PCR reactions were set up in accordance with the manufacturer's recommendations. Relative fold changes in gene expression were calculated using the  $2^{-\Delta\Delta C_T}$  method.

**2.12. Statistical Analysis.** Data are reported as mean  $\pm$  SEM. Statistical significance was assessed using either the one-way ANOVA with Tukey's test or the Tukey–Kramer multiple comparison test

when using three or more groups. To compare two groups, an unpaired Student's *t* test with Welch's correction was used. Statistical analysis was performed using GraphPad Prism 4.0.<sup>39</sup> Differences were considered significant at *p* < 0.05.

### 3. RESULTS

**3.1. 5F 203 Inhibits the Growth of Certain Malignant Breast Carcinoma Cells but Not Nonmalignant MCF-10A Breast Epithelial Cells.** To determine whether 5F 203 elicits selective cytotoxicity in malignant versus nonmalignant cells, we exposed a panel of breast cancer cells and a nonmalignant breast epithelial cell line to 5F 203 and assessed cell survival using the Alamar Blue assay. We treated estrogen receptor positive (ER<sup>+</sup>; MCF-7 and T47D) breast cancer cells, estrogen receptor negative (ER<sup>-</sup>; CRL2335, MDA-MB-231, and MDA-MB-468) breast cancer cells, and nonmalignant MCF-10A cells with 5F 203 or vehicle control (0.1% DMSO) for 72 h. Consistent with previous reports,<sup>10</sup> Figure 1A reveals that

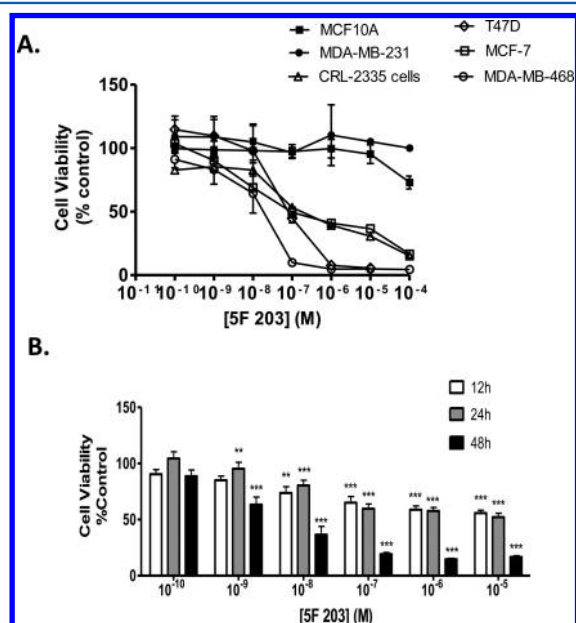


**Figure 1.** 5F 203 inhibits growth of breast cancer cells but not nonmalignant breast epithelial cells. (A) Immortalized MCF-10A nonmalignant breast epithelial cells and a panel of breast cancer cells were treated with medium containing 5F 203 (0.1 nM to 100  $\mu$ M) or 0.1% DMSO for 72 h before the Alamar Blue assay was employed as described in Materials and Methods. Data represent the mean  $\pm$  SEM of at least four independent experiments. (B) Exponentially growing malignant MDA-MB-468 cells were treated with medium containing vehicle (0.1% DMSO) or 5F 203 (0.1 nM to 10  $\mu$ M) for 12, 24, or 48 h before the Alamar Blue dye reagent was added. Fluorescence was evaluated in a microplate reader as outlined in Materials and Methods. Data represent the mean  $\pm$  SEM of at least three independent experiments and are a percentage of controls. \*\**p* < 0.01 and \*\*\**p* < 0.001 in comparison to control.

nonmalignant MCF-10A breast epithelial cells and MDA-MB-231 breast cancer cells were resistant to 5F 203 treatment, whereas the other cell lines showed varying sensitivity to 5F 203. Since MDA-MB-468 cells were the most sensitive, we evaluated whether these effects were apparent during shorter durations of 5F 203 exposure. We observed both dose- and time-dependent increases in 5F 203-induced cytotoxicity in MDA-MB-468 cells, particularly following 48 h of treatment (Figure 1B). We varied the duration of exposure to include 12,

24, and 48 h time points since the majority of gene expression studies in this report involve treatments of 24 h or less.

**3.2. 5F 203 Preferentially Increases ROS in Sensitive Breast Cancer Cells.** Many chemotherapeutic agents are known to induce cytotoxicity in tumor cells by a ROS-mediated mechanism.<sup>43</sup> To determine whether 5F 203 alters intracellular ROS levels in breast cancer cells, we treated cells with 5F 203 (6 h, 1  $\mu$ M) and then exposed them to H<sub>2</sub>DCF-DA dye before measuring ROS levels using flow cytometry. 5F 203 appeared to selectively increase ROS production in certain malignant cells in a manner that correlates with this investigational agent's ability to exhibit selective cytotoxicity. ROS levels were increased in sensitive MDA-MB-468, MCF-7, CRL2335, and T47D breast carcinoma cells, and NAC diminished 5F 203-induced ROS formation (Figure 2A,C). The superoxide dismutase/catalase mimetic EUK-134 more completely blocked 5F 203-mediated increases in ROS production in the sensitive MDA-MB-468 cells, presumably due to its more potent antioxidant actions (Figure 4B). ROS levels did not increase in the resistant MDA-MB-231 cancer cells or in MCF-10A breast epithelial cells (Figure 2A). By comparison, the BAP metabolite 1,6-benzo[*a*]pyrene quinone (1,6-BPQ) caused greater than a 2-fold increase in ROS in nontumorigenic MCF-10A cells following 2 h of exposure (Figure 2B), in agreement with a previously published study.<sup>40</sup> Therefore, AhR ligand 5F 203 selectively increased ROS production in breast cancer cells, whereas AhR ligand BAP increased ROS production more indiscriminately.

AhR target genes cytochrome P450 1A1 (CYP1A1) and cytochrome P450 1A2 (CYP1A2) have been shown to metabolize 5F 203<sup>44</sup> and directly contribute to increases in intracellular ROS levels.<sup>45</sup> To determine the role of CYP1A1 or CYP1A2 in 5F 203-induced ROS production, we pretreated cells with  $\alpha$ NF, an AhR antagonist, before exposing them to 5F 203 (Figure 2C). Our results show that 5F 203-induced ROS production was suppressed when cells were pretreated with  $\alpha$ NF (Figure 2C). We also observed an attenuation in 5F 203-mediated increases in ROS levels in MDA-MB-468 cells pretreated with the more selective AhR inhibitor, CH223191 (Figure 4B). To further confirm the AhR-dependence of 5F 203-mediated increases in ROS production during longer exposure times, we exposed AHR100 cells to 5F 203 and measured intracellular ROS levels. AHR100 cells were previously shown to resist the cytotoxic actions of 5F 203, as they are AhR ligand-unresponsive.<sup>11</sup> In Figure 2D, we show that 5F 203-mediated ROS production was substantially diminished in AHR100 cells in comparison to that in wild-type MCF-7 cells. Taken together, these data suggest that 5F 203-induced ROS production depends, at least in part, upon AhR activation.

**3.3. 5F 203 Promotes Phosphorylation of Mitogen Activated Protein Kinases p38 and JNK in Sensitive Breast Cancer Cells.** ROS-mediated MAPKs p38, ERK, and JNK modulate the anticancer activity of certain agents that have the potential to treat breast cancer.<sup>46,47</sup> Since the phosphorylation of these MAPKs is associated with their activation, we investigated whether 5F 203 promoted the phosphorylation of p38, JNK, or ERK in MDA-MB-468 and T47D breast cancer cell lines. We demonstrated that 5F 203 promotes phosphorylation of p38 and JNK in both T47D and MDA-MB-468 cells (Figure 3A,B), although less significant increases in phosphorylation of ERK (<1.5-fold increase) were observed in T47D cells (Figure 3A,B). In particular, statistically significant

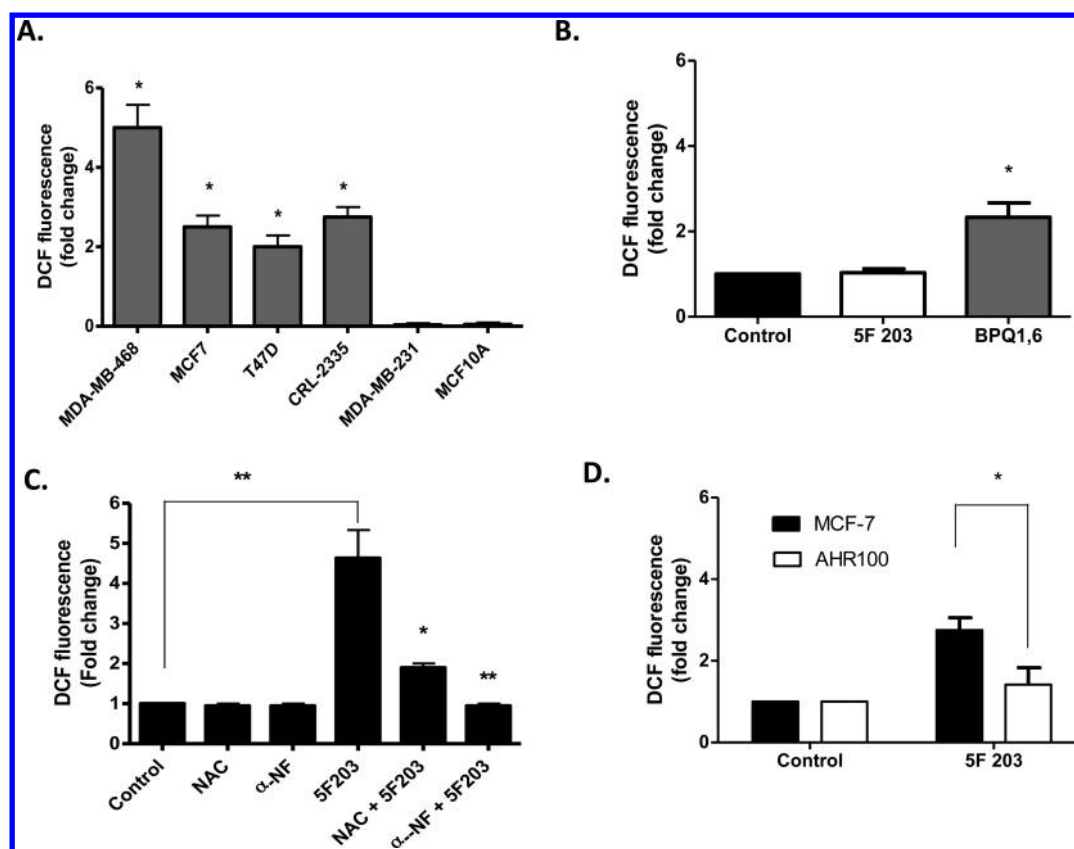


**Figure 2.** SF 203 induces AhR-dependent ROS production in sensitive breast cancer cells. (A) Sensitive and resistant cells were treated with vehicle control (0.1% DMSO) or 1  $\mu$ M SF 203 for 6 h, and intracellular ROS (DCF) levels in cells were analyzed using flow cytometry as outlined in Materials and Methods. Data represent the mean  $\pm$  SEM of at least three independent experiments performed in triplicate. \* $p$  < 0.05 compared to values for resistant cells. (B) MCF-10A cells were exposed to medium containing 0.1% DMSO, 1  $\mu$ M SF 203, or 2  $\mu$ M BPQ1,6 for 2 h before being exposed to DCF-DA dye for 15 min. Cells were harvested as described in Materials and Methods. Data represent the mean  $\pm$  SEM of at least three independent experiments performed in duplicate. \* $p$  < 0.05 compared to control. (C) MDA-MB-468 cells were treated with vehicle control (0.1% DMSO), SF 203 (1.0  $\mu$ M), or with SF 203 (6 h) following 1 h NAC (20 mM) or  $\alpha$ NF (100  $\mu$ M) pretreatment before ROS levels were analyzed via flow cytometry as outlined in Materials and Methods. Except where indicated by lines, \* $p$  < 0.05 and \*\* $p$  < 0.01 are in comparison to treatment with SF 203 alone. (D) MCF-7 and AHR100 cells were exposed to either 0.1% DMSO or 1  $\mu$ M SF 203 for 6 h before ROS levels were analyzed using flow cytometry. Data represent the mean  $\pm$  SEM of at least three independent experiments. \* $p$  < 0.05.

activation of JNK and p38 occurred in MDA-MB-468 breast cancer cells following 6 h of treatment with SF 203, which was sustained at 12 h (Figure 3A,B) and evident at 24 h of treatment (data not shown). Our data indicate SF 203 activates JNK and p38 in breast cancer cells sensitive to its cytotoxic actions.

**3.4. Inhibition of p38 and JNK Signaling Attenuates SF 203-Mediated Increases in Intracellular ROS.** A number of reports have established the role of ROS in mediating the activation of p38 and JNK signaling pathways.<sup>46,48–51</sup> To determine whether SF 203-mediated increases in ROS might be further promoted following phosphorylation of p38 or JNK, MDA-MB-468 and T47D cells were exposed for 6 h to medium containing 0.1% DMSO, JNK inhibitor SP600125, p38 inhibitor SB202190, or SF 203 with or without 1 h pretreatment with the corresponding inhibitors. We also pretreated MDA-MB-468 cells with the more selective JNK inhibitor, CC-401, followed by a 6 h treatment with SF 203. We found that p38 and JNK inhibitors significantly attenuated SF 203-mediated ROS formation (Figure 4A,B). This demonstrates that SF 203-mediated ROS generation depends, at least in part, upon p38 or JNK activation.

A positive feedback loop has been previously described in which ROS induces p38 activation to further ROS production

to sustain downstream p38 signaling in chondrocytes.<sup>52</sup> To determine whether a positive feedback loop between ROS and MAPKs (JNK or p38) exists in breast cancer cells exposed to SF 203, we pretreated cells for 30 min with SP600125 or SB202190 followed by treatment with SF 203 for 1 or 3 h in MDA-MB-468 or T47D cells, respectively. We found that at these earlier time points neither inhibitor appreciably impacted the ability of SF 203 to increase ROS production (Figure 4C), although pretreatment with these inhibitors significantly attenuated SF 203-mediated ROS formation at a later time point (6 h drug exposure) for both cell lines (Figure 4A). These results suggest that a positive feedback loop exists between ROS and JNK and between ROS and p38, which leads to the sustained activation of the respective MAPK signaling pathways in SF 203-treated cells. However, more extensive studies are needed to confirm the presence of this positive feedback loop.

**3.5. SF 203 Promotes Apoptotic Body Formation That Partially Depends on AhR, p38, or JNK Signaling in Breast Cancer Cells.** SF 203 induces apoptosis in sensitive breast cancer cells<sup>11</sup> and increases in ROS followed by activation of kinases ERK, p38, and JNK promote SF 203-mediated ovarian cancer cell death.<sup>12</sup> We visualized cells exposed to SF 203 in the presence or absence of  $\alpha$ NF or MAPK inhibitors (Figure 4D) to detect apoptosis, as evidenced



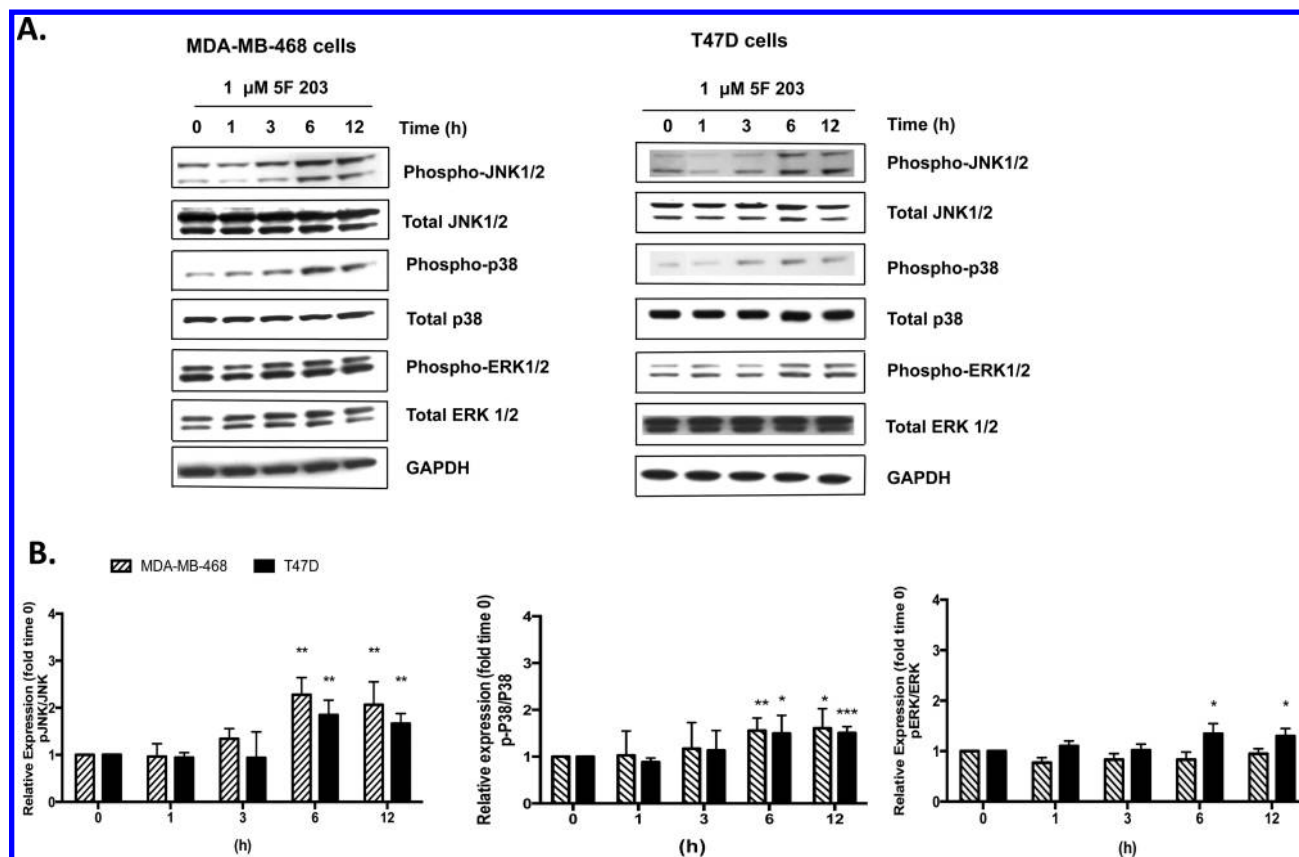


**Figure 3.** SF 203 activates JNK and p38 signaling in sensitive breast cancer cells. (A) MDA-MB-468 and T47D cells were exposed to 1  $\mu$ M SF 203 at varying time points before being harvested and analyzed by immunoblotting for JNK, p38, or ERK phosphorylation. Data is representative of three independent experiments. Gel is of a representative blot, and sections within the blot were rearranged based on treatments specified. (B) Graphs based on densitometry determination ratios for phospho-proteins relative to total proteins relative to time 0 h measurements (fold change). \* $p$  < 0.05, \*\* $p$  < 0.01, and \*\*\* $p$  < 0.001 in comparison to time 0 h measurements.

by an increase in apoptotic body formation. Consistent with a previous report, our data show that pretreatment with  $\alpha$ NF or inhibitors for p38 or JNK diminished SF 203-mediated breast cancer cell death.<sup>12</sup> Taken together, AhR, p38, and JNK signaling pathways contribute to SF 203-mediated apoptosis.

**3.6. SF 203 Induces AhR- and ROS-Dependent Phosphorylation of p38 and JNK in Breast Cancer Cells.** Because ROS production frequently results in phosphorylation of p38 and JNK, we pretreated MDA-MB-468 breast cancer cells with the antioxidant NAC to assess whether SF 203-induced activation of p38 and JNK would be attenuated. In addition, since AhR activation appears to occur prior to increasing ROS production, we also pretreated cells with  $\alpha$ NF. We found that NAC and  $\alpha$ NF inhibited SF 203-mediated JNK phosphorylation in T47D cells and p38 phosphorylation in MDA-MB-468 cells (Figures 5B,C and 6A,C). On the other hand, NAC pretreatment did not significantly suppress JNK phosphorylation in MDA-MB-468 cells (Figure 5A,C). We found that, unlike NAC, EUK-134 significantly suppressed SF 203-mediated ROS-dependent JNK phosphorylation in MDA-MB-468 cells (Figure 5D). NAC primarily demonstrates antioxidant actions, although this cysteine precursor does exhibit some reducing actions by acting as a thiol–disulfide exchanger.<sup>53</sup> By contrast, EUK-134 demonstrates powerful antioxidant actions by behaving like antioxidant enzymes superoxide dismutase and catalase. We therefore conclude that SF 203-mediated phosphorylation in these cells is due, at least in part, to increases in ROS

production. In T47D cells,  $\alpha$ NF pretreatment did not appreciably affect SF 203-mediated p38 phosphorylation (Figure 6B,C). However, pretreating cells with the highly selective AhR inhibitor CH223191 did lead to significant suppression of SF 203-mediated phosphorylation in these cells (Figure 6D). These data suggest that p38 and JNK activation occur once SF 203 triggers activation of AhR signaling and ROS.

**3.7. SF 203 Induces Single-Strand Break Formation and Oxidative DNA Damage in Sensitive Breast Cancer Cells.** Previous studies indicate that SF 203 induces dose- and time-dependent increases in DNA single-strand breaks (SSBs) in sensitive ER<sup>+</sup> MCF-7 breast cancer cells.<sup>6,35</sup> In the current study, we determined the ability of SF 203 to promote DNA SSB formation in sensitive ER<sup>+</sup> MDA-MB-468 breast cancer cells using the alkaline comet assay. Our data indicate that SF 203 induced significant dose-dependent increases in SSB formation in MDA-MB-468 cells (Figure 7A,B). NAC pretreatment only partially protected cells from SF 203-mediated SSB formation (data not shown). On the other hand, pretreatment with  $\alpha$ NF blocked SF 203-induced SSB formation (Figure 7A,B). Pretreatment with p38 and JNK inhibitors SB202190 and SP600125, respectively, also inhibited SF 203-mediated SSB formation (Figure 7C,D). These data suggest that SF 203-mediated SSB formation relies on the activation of AhR signaling as well as the activation of the p38 and JNK signaling pathways in MDA-MB-468 breast cancer cells.

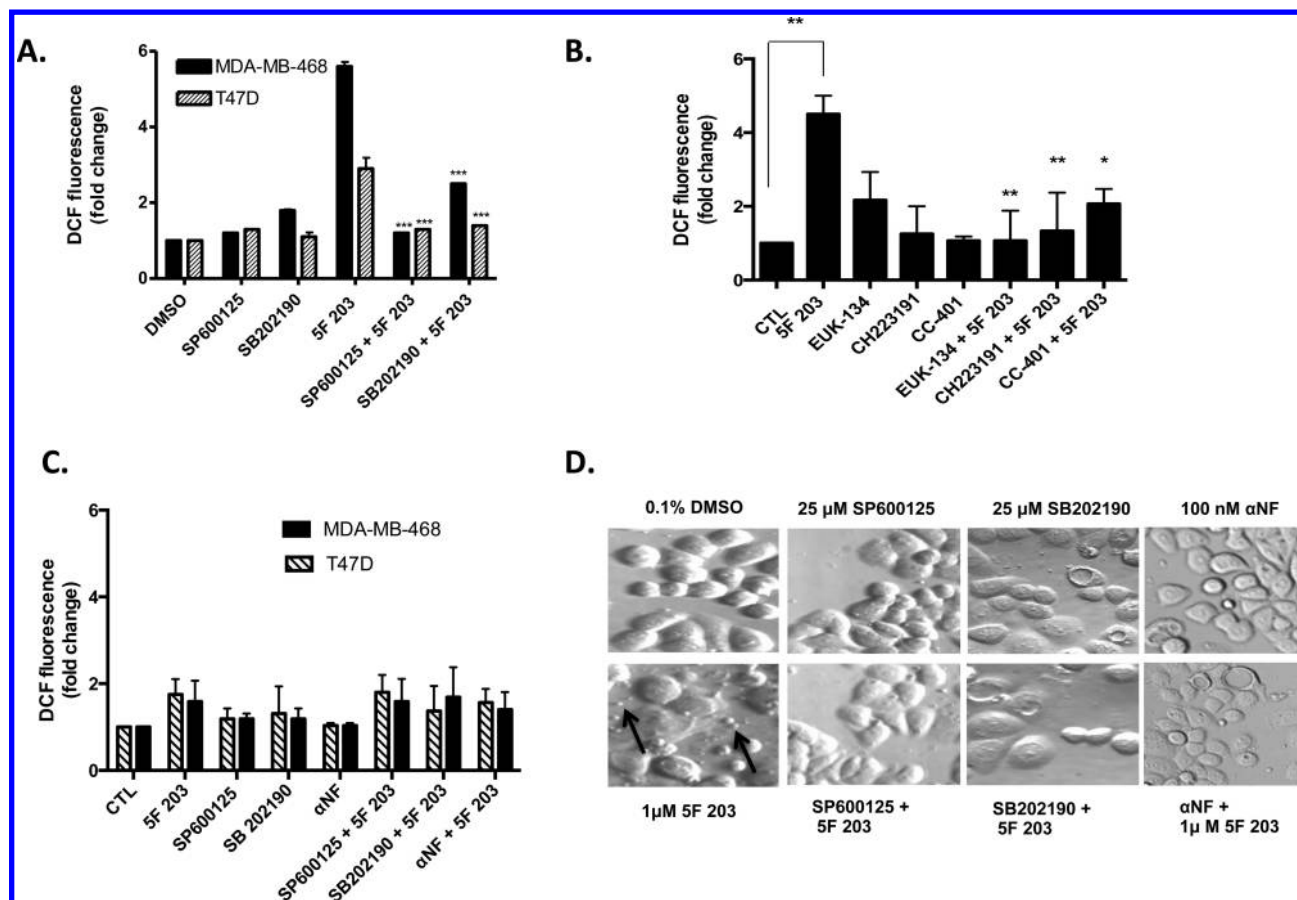


**Figure 4.** JNK and p38 contribute to SF 203-mediated increases in ROS production, and SF 203-mediated apoptotic body formation, at least partially, relies on AhR, p38, and JNK signaling in breast cancer cells. (A) MDA-MB-468 and T47D cells were pretreated for 1 h with SP600125 or SB202190 before being exposed to 1  $\mu$ M SF 203 for 6 h. Otherwise, cells were exposed to medium containing 0.1% DMSO, SF 203, or the respective inhibitors for 6 h. \*\*\* $p$  < 0.001 compared to treatment with SF 203 alone. (B) MDA-MB-468 cells were pretreated for 1 h with CC-401, CH223191, or EUK-134 before exposure to 1  $\mu$ M SF 203 for 6 h. Otherwise, cells were exposed to medium containing 0.1% DMSO, SF 203, or the respective inhibitors for 6 h. \* $p$  < 0.05 or \*\* $p$  < 0.01 compared to treatment with SF 203 alone. (C) MDA-MB-468 and T47D cells were pretreated for 30 min with SP600125 or SB202190 followed by 1 or 3 h of exposure to SF 203, respectively. Otherwise, cells were exposed to medium containing 0.1% DMSO, SF 203, or the respective inhibitors for either 1 or 3 h. ROS levels were evaluated using flow cytometry. (D) MDA-MB-468 breast cancer cells were exposed to SF 203 (6 h) with or without pretreatments with 100 nM  $\alpha$ NF, 25  $\mu$ M p38 SB202190, or 25  $\mu$ M SP600125 (1 h) before cells were visualized by relief contrast microscopy. Magnification, 200 $\times$ . Apoptotic bodies are indicated by arrows.

ROS can cause direct damage and oxidation of DNA. Some common oxidative DNA damage lesions include 8-oxodG, thymine glycol, and 5-hydroxymethyluracil. 8-OxodG has been extensively studied and has been found to play a major role in the induction of spontaneous mutations that result in DNA damage. To further characterize the nature of the SSBs that are induced by SF 203 and more clearly elucidate the role of SF 203-induced oxidative stress in DNA damage, we used HPLC-ECD to measure the levels of oxidative DNA damage (8-oxodG/dG) in MDA-MB-468 cells after treatment with 1  $\mu$ M SF 203 for 12 h (Figure 8A). SF 203 induced a greater than 3-fold increase in 8-oxodG/dG levels in MDA-MB-468 cells as compared to that in the negative control (0.1% DMSO) and to a greater extent than that in our positive control (100  $\mu$ M BSO + 500  $\mu$ M H<sub>2</sub>O<sub>2</sub>). A 2-fold increase in oxidative DNA damage is the maximal amount typically detected in nature.

We also used a flow cytometry based-method (OxyDNA assay) to evaluate oxidative DNA damage in certain cells treated with SF 203. The OxyDNA assay enables one to detect a shift in fluorescence peaks (due to FITC-bound protein conjugate linked to 8-oxoguanine) to determine the extent of oxidative DNA damage. We detected a greater than 2-fold

increase in oxidative DNA damage in MDA-MB-468 cells using this assay in cells exposed to SF 203 and a 1.5-fold increase in cells exposed to BSO/H<sub>2</sub>O<sub>2</sub> (Figure 8B). This further confirms that SF 203 induces oxidative DNA damage in sensitive breast cancer cells.

To investigate the role of intracellular glutathione in SF 203-induced cytotoxicity, we treated MDA-MB-468 cells with 1  $\mu$ M SF 203 for 12 h, and total intracellular glutathione levels were measured using an MCB ApoAlert glutathione detection assay. Glutathione levels were significantly decreased in MDA-MB-468 cells (Figure 8C). Such data further corroborate the ability of SF 203 to modulate oxidative stress levels within susceptible cells.

We next evaluated the DNA damaging capacity of AhR agonist BAP and compared it with SF 203 in MCF-10A breast epithelial cells using the flow cytometry method. We found that BAP induced dose-dependent increases in oxidative DNA damage in these cells (Figure 8D). In contrast, SF 203 caused no significant increase in oxidative DNA damage in these breast epithelial cells. This is in agreement with the observation that cell viability in these cells is unaffected by even prolonged exposure to high concentrations of SF 203 (Figure 1A). These



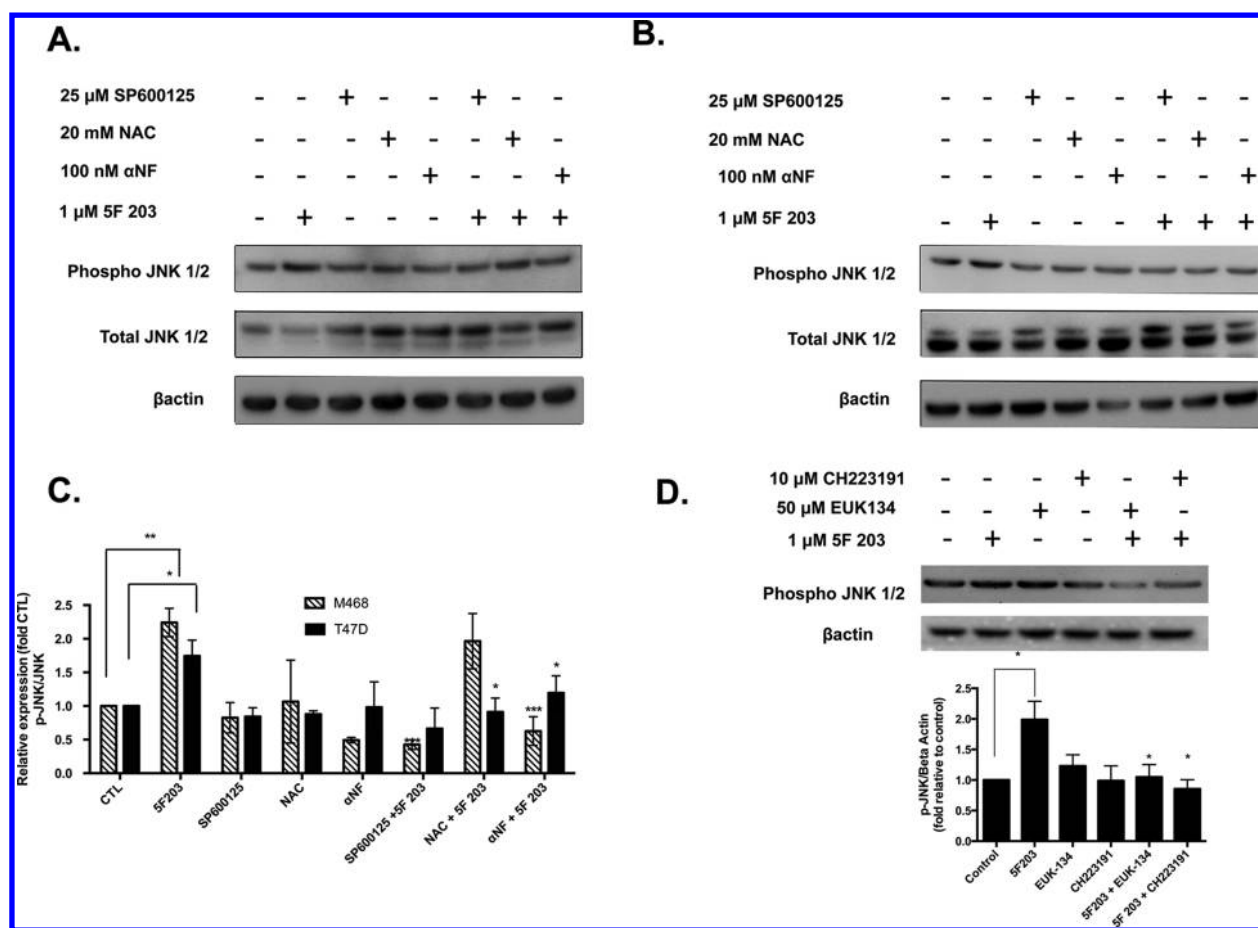


**Figure 5.** AhR antagonists suppress SF 203-mediated JNK phosphorylation in breast cancer cells. (A) MDA-MB-468 and (B) T47D cells were treated with 0.1% DMSO,  $\alpha$ NF, NAC, SP600125, or 1  $\mu$ M SF 203 for 6 h or were pretreated for 1 h with 100 nM  $\alpha$ NF, 20 mM NAC, or 25  $\mu$ M SP600125 before being exposed to 1  $\mu$ M SF 203 for 6 h. Following treatment, cells were lysed, and protein content was determined and resolved using western blotting as described in Materials and Methods. Gel is of a representative blot. (C) Data is representative of three independent experiments. Graphs based on arbitrary units of ratios densitometry determinations for phospho-proteins relative to total protein and used to quantify the extent of activation. (D) MDA-MB-468 cells were exposed to SF 203 (6 h) with or without EUK-134 or CH223191 pretreatment, and western blotting analysis was performed along with densitometry readings. Data represent the mean of at least three independent experiments; bars, SEM. Except where indicated by lines, \* $p$  < 0.05, \*\* $p$  < 0.01, and \*\*\* $p$  < 0.001 compared to cells exposed to SF 203 only.

data demonstrate SF 203 induces oxidative DNA damage in breast cancer cells but not in nonmalignant breast epithelial cells, unlike AhR agonist and procarcinogen BAP.

### 3.8. SF 203 Differentially Modulates Human Oxidative Stress Associated Genes in Certain Breast Cancer Cells.

Small molecules that modulate ROS frequently perturb downstream genes that ultimately regulate oxidative stress. We therefore used the human oxidative stress and antioxidant defense RT<sup>2</sup> profiler PCR array to examine the expression of 84 oxidative stress-related genes in CRL 2335, MCF-7, and MDA-MB-468 cells exposed to 1  $\mu$ M SF 203 for 24 h. SF 203 appeared to differentially and significantly modulate the expression of several genes associated with oxidative stress response (Table 1). In particular, *cytoglobin* (CYGB) gene expression increased significantly in two of these cell lines. The increase in CYGB expression in CRL2335 cells did not quite reach statistical significance. On the other hand, induction was robust in MCF-7 and MDA-MB-468 breast cancer cells, with 24- and 67-fold increases, respectively. To a much lesser extent, SF 203 modulated the expression of at least four distinct genes per cell line. In general, SF 203 modulated the expression of oxidative stress-related genes to favor anticancer activity. For instance, SF 203 induced the expression of *apolipoprotein E*

(APOE), a breast differentiation factor, in MDA-MB-468 cells.<sup>54</sup> In MCF-7 cells, SF 203 increased the expression of the *glutathione peroxidase* gene (GPX2), an inhibitor of cancer cell migration and invasion.<sup>55</sup> In CRL 2335 cells, SF 203 significantly downregulated the expression of *interactor protein for cytohesin exchange factors 1* (IPCEF1), which promotes cell migration.<sup>56</sup> Thus, the differential gene profile elicited from SF 203 treatment in different breast cancer cell lines implies that differential response to SF 203 is complex and cell context-dependent. These data further support our hypothesis that oxidative stress plays a prominent role in the mechanism of anticancer action for SF 203.

### 3.9. SF 203-Mediated Induction of CYGB Expression Parallels Relative Breast Cancer Cell Sensitivity.

To determine the relationship between CYGB gene induction and cell sensitivity, we used single-gene qPCR primer assays to compare CYGB gene induction in a panel of breast cancer cells, including MDA-MB-231 cells that are known to be resistant to SF 203. We observed that CYGB induction (>50-fold relative to untreated control) was most robust in MDA-MB-468 cells, which were most sensitive to SF 203 (Figure 9A). On the other hand, no appreciable upregulation of CYGB expression was evident in MDA-MB-231 cells, the most resistant to SF 203-

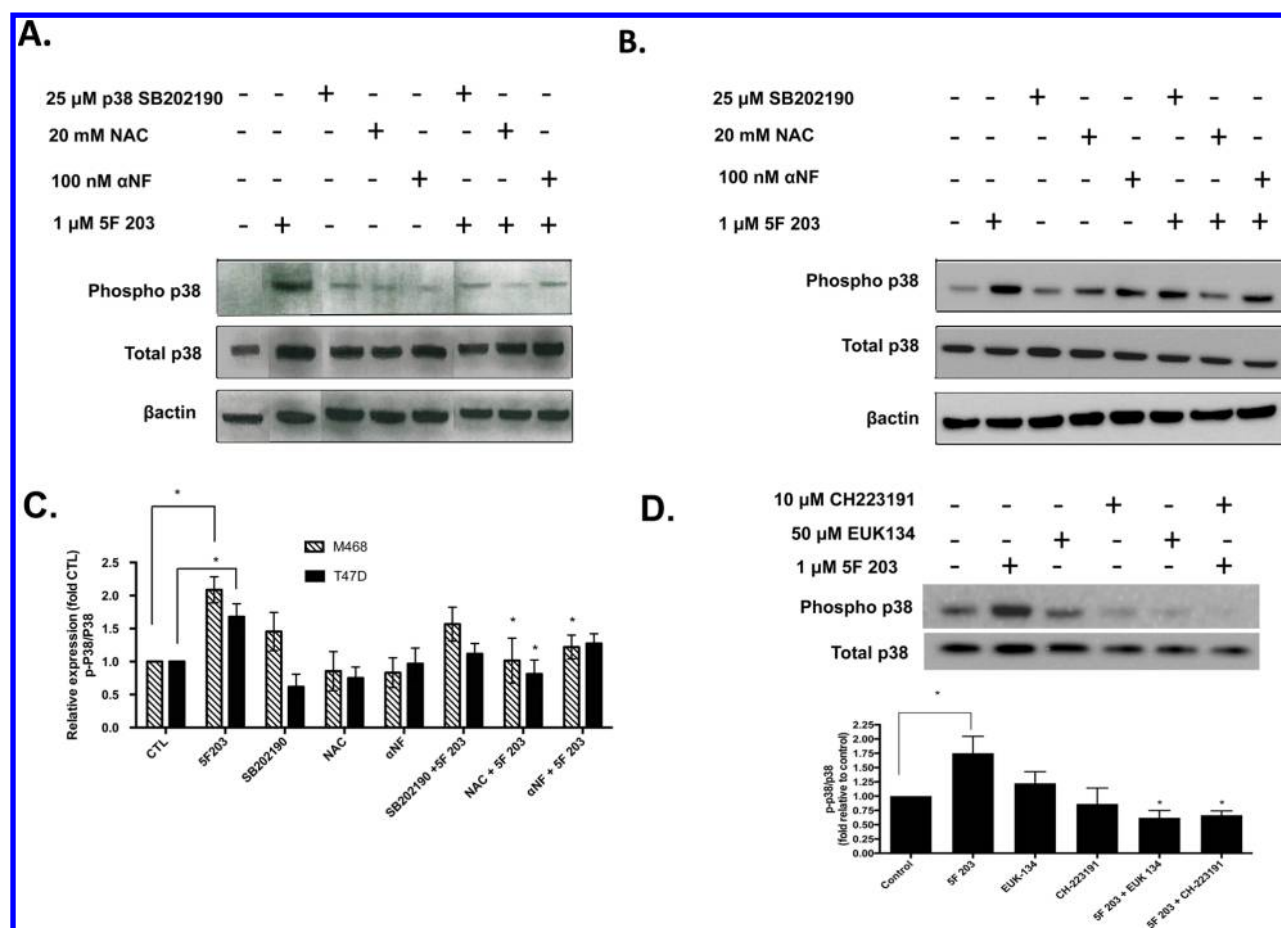


**Figure 6.** AhR antagonists suppress SF 203-mediated p38 phosphorylation in breast cancer cells. (A) MDA-MB-468 and (B) T47D cells were treated with 0.1% DMSO,  $\alpha$ NF, NAC, SB202190, or 1  $\mu$ M SF 203 for 6 h or were pretreated for 1 h with  $\alpha$ NF (100 nM), NAC (20 mM), or SB202190 (25  $\mu$ M) before being exposed to 1  $\mu$ M SF 203 for 6 h. Following treatment, cells were lysed, and protein content was determined and resolved using western blotting as described in Materials and Methods. Gel is of a representative blot, and sections within the blot were rearranged based on treatments specified. (C) Data is representative of three independent experiments. Graphs based on arbitrary units of ratios densitometry determinations for phospho-proteins relative to total protein and used to quantify the extent of activation. (D) MDA-MB-468 cells were exposed to SF 203 (6 h) with or without EUK-134 or CH223191 pretreatment, and western blotting analysis was performed along with densitometry readings. Data represent the mean of at least three independent experiments; bars, SEM. Except where indicated by lines, \* $p$  < 0.05 compared to cells exposed to SF 203 only.

induced cytotoxicity (Figure 1A).<sup>10</sup> In CRL 2335 cells, *CYGB* expression was upregulated approximately 3-fold compared to that in untreated controls. These cells demonstrated moderate sensitivity to the cytotoxic effects of SF 203 (Figure 1A). In MCF-7 cells, *CYGB* expression was upregulated 24-fold relative to the untreated control. These results are consistent with the results of the PCR-array (Table 1) and suggest that *CYGB* induction may serve as a biomarker for sensitivity to SF 203.

**3.10. SF 203 Induces Greater Induction of Cytoglobin than Doxorubicin or the DNA Methyltransferase Inhibitor 5-Aza-2'-deoxycytidine.** To distinguish whether *CYGB* induction is a nonspecific response to treatment with anticancer agents and/or AhR activation, as opposed to a specific response to SF 203, we compared *CYGB* expression after exposure to several agents. Such agents included anticancer agent doxorubicin (Dox); the DNA methyltransferase inhibitor 5-Aza, shown previously to reactivate *CYGB*;<sup>57</sup> and 1,6-BPQ. All agents were used at concentrations that were within the range known to elicit cytotoxicity in the selected breast cancer cells or MCF-10A cells. In MDA-MB-468 cells, we observed that SF 203 significantly upregulated *CYGB* expression, whereas 5-Aza caused a less profound, although

significant, increase in *CYGB* expression (Figure 9B). Dox caused an increase in *CYGB* expression, although it was not statistically significant. Notably, no significant *CYGB* gene induction occurred in any of the cells that were exposed to 1,6-BPQ. To determine whether SF 203 modulates *CYGB* gene expression at the transcriptional level, and even during shorter durations of exposure and at lower concentrations, MDA-MB-468 cells were treated with SF 203 (250 nM, 12h) in the presence or absence of actinomycin D (1 h pretreatment). We then analyzed samples using quantitative real-time PCR analysis. We used 250 nM since SF 203 exhibited a capacity to induce *CYGB* expression even at concentrations as low as 100 nM and less cytotoxicity was evident following 12 h at this concentration. Our data indicate that actinomycin D blocks the ability of SF 203 to induce *CYGB* expression (Figure 9C). These data suggest SF 203 induces *CYGB* more specifically than chemotherapeutics such as Dox and that SF 203 promotes *CYGB* upregulation at the transcriptional level.

**3.11. AhR, p38, and JNK Contribute to SF 203-Mediated Cytoglobin Induction in MDA-MB-468 Breast Cancer Cells.** Since *CYGB* has been described as an oxidative stress-responsive gene<sup>58</sup> with tumor suppressor gene func-

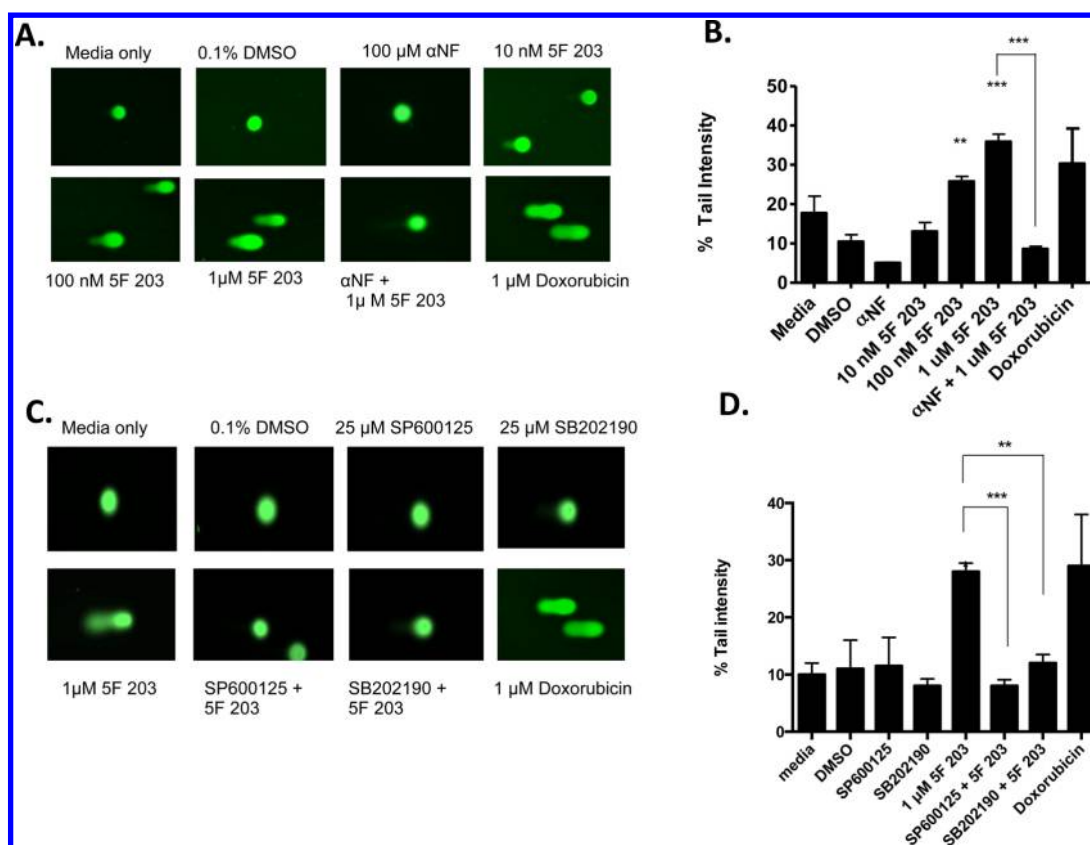


**Figure 7.** SF 203 induces SSBs in sensitive breast cancer cells. (A, B), Cells were exposed for 12 h to medium only or medium containing 0.1% DMSO, SF 203 (10–1000 nM), doxorubicin (1  $\mu$ M),  $\alpha$ NF (100  $\mu$ M), or SF 203 (1  $\mu$ M) following pretreatment with  $\alpha$ NF (1 h). SSBs were evaluated using the alkaline comet assay as outlined in Materials and Methods. Except where indicated by lines,  $**p < 0.01$  and  $***p < 0.001$  compared to DMSO-exposed (control) cells. Data represent the mean  $\pm$  SEM of at least three independent experiments. (C, D) Cells were exposed to medium only or medium containing 0.1% DMSO, SP600125, SB202190, or SF 203 (1  $\mu$ M, 12 h) in the presence or absence of SP600125 (1 h) or SB202190 pretreatment (1 h). Following treatment, SSBs were evaluated using the alkaline comet assay as detailed in Materials and Methods. Except where indicated by lines,  $**p < 0.01$  and  $***p < 0.001$  compared to DMSO-exposed (control) cells. Data represent the mean  $\pm$  SEM of at least three independent experiments.

tion,<sup>57</sup> we investigated whether inhibition of p38, AhR, or JNK activation would interfere with SF 203-mediated induction of CYGB. Our data show that pretreatment with SB202190,  $\alpha$ NF, or SP600125 diminished the ability of SF 203 to increase CYGB expression in MDA-MB-468 cells (Figure 9D). We further confirmed that AhR and JNK pathways participate in SF 203-mediated induction of CYGB expression by pretreating cells with CH223191 or CC-401, respectively (Figure 9E). Since EUK-134 blocks SF 203-mediated increases in ROS, we pretreated cells with this antioxidant and determined that SF 203-mediated induction of CYGB was also diminished (Figure 9E). We also determined that SF 203 was unable to increase CYGB expression in AHR100 cells (Figure 9F) to further confirm that the AhR signaling pathway plays a role SF 203-mediated CYGB upregulation. Taken together, the AhR, ROS, p38, and JNK signaling pathways participate in CYGB regulation.

#### 4. DISCUSSION

In this study, we demonstrate that SF 203 increases intracellular ROS, which culminates in DNA damage in certain breast cancer cells. SF 203-mediated induction of ROS and oxidative DNA damage occurs exclusively in breast cancer cells that demonstrate sensitivity to this investigational agent (Figures 2A and 8A,B). We found no appreciable increase in either ROS or

oxidative DNA damage in resistant cells following SF 203 treatment, including MCF-10A nonmalignant breast epithelial cells (Figures 2A and 8D). On the other hand, MCF-10A cells were susceptible to ROS formation and oxidative DNA damage when exposed to 1,6-BPQ and BAP, respectively (Figures 2B and 8D).<sup>40,59,60</sup> Although 1,6-BPQ is not a designated ultimate carcinogen, it has been shown to stimulate MCF10A cell proliferation and may promote malignant transformation due to its propensity to increase ROS levels in these cells.<sup>40</sup> We observed no appreciable reduction in the viability of MCF-10A cells exposed to high concentrations of SF 203 (>50  $\mu$ M). In contrast to many AhR agonists, our data indicate that SF 203 displays selective cytotoxicity, which is in agreement with previous studies (Figure 1A).<sup>11,35,61–63</sup>

The attenuation of SF 203-induced ROS production in AHR100 cells and its inhibition in MDA-MD-468 cells following  $\alpha$ NF or CH223191 pretreatment indicate that SF 203-induced ROS production is AhR-dependent (Figures 2C,D, and 4B). Since AhR antagonists such as  $\alpha$ NF and even CH223191 frequently impact CYP1 activity and most CYP1 inhibitors also act by binding to AhR, we could not conclusively rule out the possibility that SF 203-mediated modulation in intracellular ROS levels occurred in part due to actions of CYPs as opposed to AhR. Interestingly,  $\alpha$ NF exhibited a superior ability to suppress SF 203-mediated CYP1 induction compared



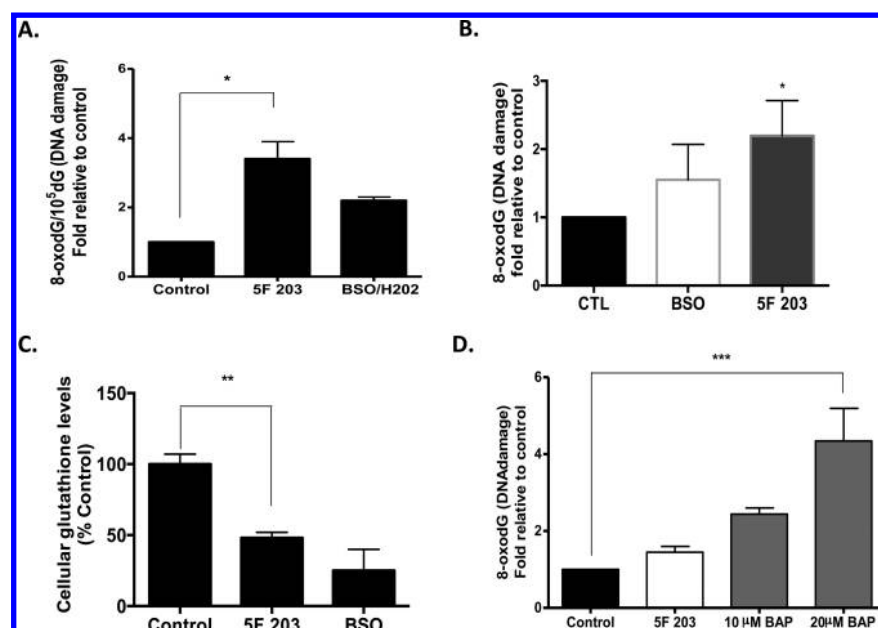


**Figure 8.** SF 203 induces oxidative DNA damage in MDA-MB-468 breast cancer but not MCF-10A breast epithelial cells. (A) Oxidative DNA damage was determined by measuring the levels of 8-oxodG/10<sup>5</sup> dG. MDA-MB-468 cells were treated with 1 μM SF 203 for 12 h or pretreated for 18 h with 100 μM BSO followed by the addition of 500 μM H<sub>2</sub>O<sub>2</sub> in the medium for 30 min. Data represent the mean ± SEM of at least three independent experiments. \**p* < 0.05. (B) Oxidative DNA damage was also determined using the OxyDNA assay with the treatments described in (A). Data represent the mean ± SEM of at least three independent experiments performed in duplicate. \**p* < 0.05 compared to control. (C) Cells were exposed to medium containing 0.1% DMSO (negative control, 12h), 1 μM SF 203 (12 h), or buthionine sulfoxide (BSO, 100 mM, 18 h) before the glutathione assay was performed. \*\**p* < 0.01. (D) MCF-10A breast epithelial cells were exposed to 0.1% DMSO, SF 203 (1 μM), or benzo[*a*]pyrene (10 and 20 μM) for 24 h as outlined in Materials and Methods. Data represent the mean ± SEM of at least three independent experiments. \*\*\**p* < 0.001.

**Table 1.** SF 203-Mediated Modulation of Oxidative Stress-Responsive Genes in Breast Cancer Cells<sup>a</sup>

cell line	gene name	fold	known or potential regulation/role	GI <sub>50</sub> <sup>c</sup>
CRL2335	cytoglobin (CYGB)	↑6.17 <sup>b</sup>	tumor suppressor, oxygen sensing	390 nM
	prostaglandin-endoperoxide synthase 2 (PTGS2)	↑4.85	inflammation and prostaglandin biosynthesis	
	keratin 1 (KRT1)	↓4.04	Differentiation marker	
	interaction protein for cytohesin exchange factors 1 (IPCEF1)	↓6.83	binds to cytohesin	
MCF7	CYGB	↑24.05	stated above	110 nM
	glutathione peroxidase 2 (GPX2)	↑3.33	selenium-dependent glutathione peroxidase	
	chaperone for superoxide dismutase (CCS)	↑3.04	delivers Cu to copper/zinc superoxide dismutase	
	methionine sulfoxide reductase A (MSRA)	↓5.24	repairs oxidative damage to proteins	
	aldehyde oxidase I (AOX1)	↓3.20	produces hydrogen peroxide	
MDA-MB-468	CYGB	↑67.16	stated above	31 nM
	apolipoprotein E (APOE)	↑4.33	primary apoprotein of chylomicrons	
	sulfiredoxin 1 homologue (SRXN)	↑3.25	antioxidant; reduces oxidative modifications	
	thyroid peroxidase (TPO)	↓16.0	plays major role in thyroid gland function	
	epoxide hydrolase 2 (EPHX2)	↓3.74	detoxifying enzyme; hydrolyzes epoxides	

<sup>a</sup>Cells were exposed to media containing 0.1% DMSO or 1 μM SF 203 for 24 h before being harvested and extracting RNA. RNA extracts were then evaluated for gene expression using a human oxidative stress-specific PCR array. Values represent means of three independent experiments and are statistically significant *p* < 0.05. <sup>b</sup>Value is not quite statistically significant, with *P* = 0.06. <sup>c</sup>An Alamar Blue assay was performed, and the GI<sub>50</sub> was determined (the concentration of SF 203 needed to inhibit 50% of the growth of cells) following exposure for 72 h. The symbols ↑ and ↓ indicate up- and downregulated, respectively.

to that with CH223191 (data not shown). It is therefore quite feasible that increases in ROS production following SF 203 exposure involves combined actions of AhR and CYP1.

We showed that treatment with SF 203 is associated with increased phosphorylation of p38 and JNK in both T47D and MDA-MB-468 breast cancer cells (Figure 3). JNK and p38

phosphorylation is frequently associated with apoptosis and differentiation.<sup>64,65</sup> Interestingly, SF 203 activated ERK in T47D cells, although to a lesser extent than p38 and JNK, whereas no appreciable activation was detected in the MDA-MB-468 cells. ERK activation was previously observed in IGROV-1 ovarian cancer cells, and these cells demonstrate

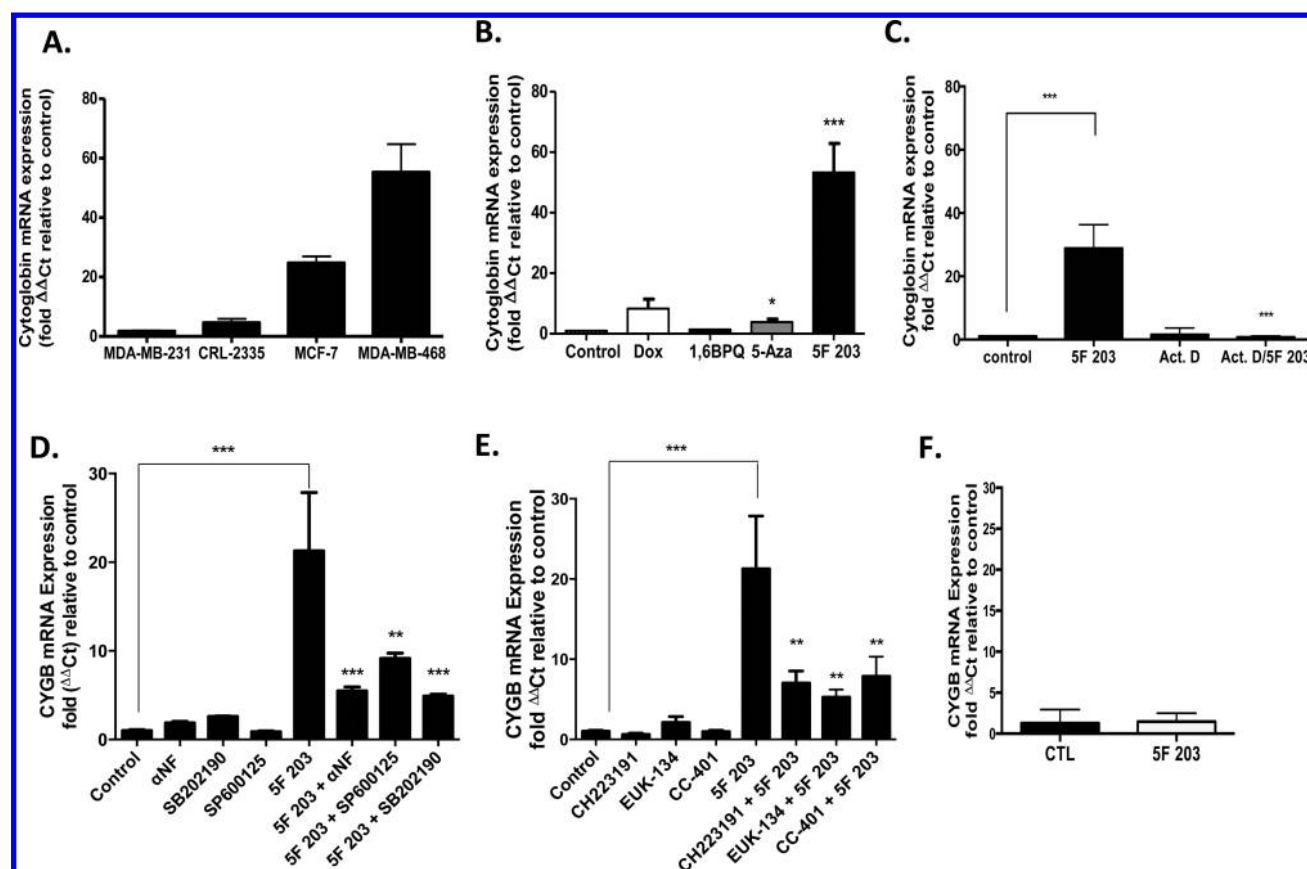


**Figure 9.** SF 203 induces cytoglobin expression in sensitive breast cancer cells, which depends, in part, on AhR, p38, or JNK signaling. (A) MDA-MB-468, MCF-7, CRL2335, and MDA-MB-231 cells were exposed for 24 h to medium containing 0.1% DMSO or 1  $\mu$ M SF 203. RNA was extracted, and gene expression was evaluated using real-time PCR as outlined in Materials and Methods. Data represent the mean  $\pm$  SEM of at least three independent experiments. (B) MDA-MB-468 breast cancer cells were exposed to medium containing 0.1% DMSO, 1  $\mu$ M SF 203, 10  $\mu$ M 5-aza-2'-deoxycytidine (5-Aza), 1  $\mu$ M doxorubicin (Dox), or 5  $\mu$ M 1,6-BPQ for 24 h. RNA was extracted from cells, and cytoglobin mRNA expression was determined in accordance with Materials and Methods. \* $p$  < 0.05 and \*\*\* $p$  < 0.001 compared to control. Data represent the mean  $\pm$  SEM of at least three independent experiments performed in triplicate. (C) MDA-MB-468 breast cancer cells were exposed to medium containing 0.1% DMSO, 250 nM SF 203, 5  $\mu$ M actinomycin D (Act. D), or SF 203 in combination with Act. D for 12 h before cells were harvested, RNA was extracted, and mRNA expression was determined as outlined in Materials and Methods. Data represent the mean  $\pm$  SEM of at least three independent experiments. \*\*\* $p$  < 0.001 as designated by line comparison. Otherwise, \*\* $p$  < 0.01 or \*\*\* $p$  < 0.001 compared to SF 203 only. (D) MDA-MB-468 breast cancer cells were exposed for 12 h to medium containing 0.1% DMSO, 100 nM  $\alpha$ NF, 25  $\mu$ M SP600125, 25  $\mu$ M p38 SB202190, 1  $\mu$ M SF 203 in the presence or absence of inhibitor pretreatments before gene expression was evaluated using quantitative-PCR in accordance with Materials and Methods. \*\*\* $p$  < 0.001 as designated by line comparison. Otherwise, \*\* $p$  < 0.01 or \*\*\* $p$  < 0.001 compared to cells exposed to SF 203 only. Data represent the mean  $\pm$  SEM of three independent experiments. (E) MDA-MB-468 cancer cells were exposed for 12 h to medium containing 0.1% DMSO, 10  $\mu$ M CH223191, 10  $\mu$ M CC-401, 50  $\mu$ M EUK-134, or 1  $\mu$ M SF 203 in the presence or absence of inhibitor or antioxidant pretreatments before gene expression was evaluated using quantitative-PCR in accordance with Materials and Methods. \*\*\* $p$  < 0.001 as designated by line comparison. Otherwise, \*\* $p$  < 0.01 compared to cells exposed to SF 203 only. (F) AHR100 cells were exposed to 0.1% DMSO or 1  $\mu$ M SF 203 for 12 h before undergoing cytoglobin mRNA expression analysis using quantitative PCR analysis. Data represent the mean  $\pm$  SEM of three independent experiments.

similar sensitivity to SF 203 as that of T47D cells.<sup>12,44</sup> In this study, we show that SF 203-mediated ROS production promoted p38 and JNK phosphorylation in both T47D and MDA-MB-468 cells. Additionally, AhR inhibition suppressed SF 203-mediated phosphorylation of JNK or p38 in these cells to imply that AhR serves as an upstream regulator of these kinases (Figures 5 and 6). These data suggest SF 203-mediated AhR signaling activation increases intracellular ROS to promote JNK and p38 phosphorylation in breast cancer cells.

Both JNK and p38 have been previously shown to engage in cross-talk with the AhR signaling pathway<sup>29,66</sup> to regulate common downstream targets. We found that pretreatment with JNK or p38 inhibitors significantly attenuated SF 203-mediated ROS formation in MDA-MB-468 cells after 6 h of exposure (Figure 4 A,B). The inability of the p38 or JNK inhibitors to

impede SF 203-mediated ROS increases following shorter treatment durations suggests the presence of a positive feedback loop similar to what has been previously described in articular chondrocytes.<sup>52</sup> Such a positive feedback loop has been proposed between ROS–JNK–p53 in previous reports not only to result in sustained JNK activation in and of itself<sup>67</sup> but also to promote autophagy<sup>68</sup> or apoptosis.<sup>69</sup> However, more extensive investigations are warranted to verify the presence of a positive feedback loop.

A number of studies show that certain agents increase ROS, leading to ROS-mediated p38 and JNK signaling activation to promote breast cancer cell death.<sup>70,71</sup> However, fewer reports describe p38- or JNK-mediated signaling as part of the molecular mechanism of drug-induced DNA damage.<sup>1,21</sup> We and others have previously demonstrated a link between AhR

signaling and the ability of SF 203 to mediate DNA damage.<sup>11,35</sup> In the current study, we found that pretreatment with SB202190, SP600125, or  $\alpha$ NF completely inhibited SF 203-induced SSB formation (Figure 7). These data suggest SSB formation relies, at least in part, on activation of AhR, p38, and JNK signaling pathways.

Since SF 203 induces oxidative stress, it is also quite plausible that this small molecule activates the nuclear factor erythroid-derived receptor 2-like2 (Nrf2) signaling pathway. Indeed, AhR agonists that increase ROS production may indirectly trigger this antioxidant pathway due to a cell-adaptive response. More directly, it is possible that SF 203 may promote the recruitment of the AhR to the xenobiotic response element found on the promoter of *Nrf2* via a feed-forward mechanism that permits ROS to modulate AhR expression. Nrf2 and AhR signaling pathways frequently cross-talk to transmit responses from AhR agonists.<sup>72</sup>

Differential cellular responses to AhR agonists may be attributed to structural differences in the ligands, the nature of any resultant metabolites, or differences in the molecular mechanisms by which either the ligands or metabolites activate AhR signaling. Toxic and chemopreventive AhR ligands have been shown to activate AhR signaling via distinct molecular mechanisms, which produce disparate cellular fates.<sup>73</sup> For example,  $\beta$ -naphthoflavone promotes the recruitment of pol II and histone acetylases to the *CYP1A1* promoter, whereas the chemopreventive agent diindolymethane activates AhR signaling without pol II recruitment or histone acetylase activation.<sup>74</sup> Selective AhR modulators (SAhRMs) proposed by Safe and colleagues were designed to promote the activation of AhR signaling in a manner that is associated with anticancer activity while lacking the propensity to induce hepatic *CYP1A1*-dependent activity and other toxic responses commonly found with 2,3,7,8-tetrachlorodibenzodioxin (TCDD).<sup>75</sup>

Certain AhR agonists have previously been reported to inhibit the growth of human breast cancer cells.<sup>76,77</sup> TCDD and other AhR agonists are able to trigger AhR activation to promote breast epithelial cell differentiation and inhibit breast cancer cell growth, metastases, and invasion.<sup>77</sup> AhR activation has been shown to initiate ER degradation and inhibit estrogen sensitive gene induction.<sup>78,79</sup> Additionally, activation of AhR signaling has been proposed as a viable approach to treat ER<sup>-</sup> breast cancer.<sup>80</sup> In our study, both ER<sup>+</sup> T47D and ER<sup>-</sup> MDA-MB-468 breast cancer cells showed sensitivity to SF 203, and these cells are indeed responsive to AhR activation.

In this study, we found that SF 203 promoted a differential gene expression profile among the breast cancer cell lines, which suggests that each cell line responds to SF 203 by both related and distinct molecular mechanisms (Table 1). Our data reveal induced *CYGB* expression as a common event among certain breast cancer cells and parallels their relative sensitivity to SF 203. This is supported by the lack of *CYGB* induction in the resistant MDA-MB-231 cells and the robust *CYGB* induction in the most sensitive MDA-MB-468 cell line (Figure 9A and Table 1). We speculate that there are yet to be discovered mechanisms that determine cell responsiveness to SF 203. Indeed, cell sensitivity to the antitumor AhR agonist, aminoflavone, appeared to be linked to endogenous sulfo-transferase activity levels.<sup>81</sup> More recently, breast cancer cells were sensitized to aminoflavone when combined with histone deacetylase inhibitor vorinostat.<sup>82</sup>

We determined that *CYGB* upregulation does not occur solely in response to cytotoxicity, as *CYGB* induction in cells

exposed to either the DNA methyltransferase inhibitor, 5-Aza, or anticancer agent doxorubicin was less pronounced as compared with that in cells exposed to SF 203 (Figure 9B). Since SF 203 induces *CYGB* expression to a greater extent than 5-Aza, it is likely that alternative epigenetic pathways contribute to *CYGB* upregulation in addition to those regulating DNA methyltransferases. The inability of the BAP metabolite 1,6-BPQ to induce *CYGB* expression suggests that AhR agonists with a greater propensity to demonstrate deleterious rather than beneficial effects may be readily identified via gene expression profiling studies such as the one we used in the present report. These data suggest that *CYGB* upregulation is linked to the ability of SF 203 to display anticancer action, although more extensive investigations are warranted to establish *CYGB* as a viable target of SF 203 responsiveness.

In addition to tumor suppressor action, *CYGB* may demonstrate a cytoprotective role to ultimately lessen the deleterious effects SF 203-mediated oxidative stress and ensuing DNA damage in cancer cells. In comparison to wild-type rats, *CYGB*-overexpressing transgenic rats exhibit preservation of kidney integrity and reduced fibrosis, which coincides with a decrease in urinary 8-hydroxy-2'-deoxyguanosine (8-OHdG) excretion indicative of decreased oxidative stress.<sup>83</sup> Additionally, during ischemia, *CYGB* protects kidney fibroblasts from the damaging actions of oxidative stress.<sup>84</sup> More recently, a dichotomous role for *CYGB* has been demonstrated in lung adenocarcinoma cells.<sup>85</sup> According to this study, during normoxia and in the absence of oxidative stress, *CYGB* conferred tumor suppressor action. However, during oxidative stress or hypoxia, *CYGB*-overexpressing lung adenocarcinoma cells demonstrated enhanced survival and invasion in comparison to that of wild-type cells. Moreover, the mitochondrial inner membrane anion carrier *uncoupling protein 2* (*UCP-2*) negatively regulates ROS and impedes apoptosis, and *UCP-2* was found to be downregulated in breast cancer cells transfected to overexpress *CYGB*.<sup>57</sup> Indeed, the behavior of *CYGB* appears to depend on cell context and cellular microenvironment.

Kovacic and Somanathan demonstrated that aromatic amines participate in redox cycling to produce electron transfer hydroxylamine metabolites that promote ROS formation to destroy cancer cells.<sup>86,87</sup> Wang and Guengerich identified CYP-generated hydroxylamine and nitrenium species of SF 203.<sup>62</sup> Our attempts to confirm the identity of the SF 203 metabolites that contribute to increases in ROS production have been unsuccessful thus far. However, we believe that the CYP-generated hydroxylamine and nitrenium species of SF 203 represent the most plausible metabolites responsible for producing ROS that lead to DNA damage in our current study. Indeed, we found that a direct causal relationship exists between the ability of SF 203 to activate p38 and JNK signaling following its CYP-catalyzed conversion into hydroxylamine and nitrenium species, which involves electron transfer redox cycling. This redox cycling promotes DNA adduct formation, which produces DNA single-strand breaks.

Our data reveal that *CYGB* expression is regulated, at least in part, by the AhR, p38, and JNK signaling pathways, as pharmacological inhibition of each of these pathways attenuated its expression (Figure 9D,E). The inability of SF 203 to induce significant *CYGB* expression in AHR100 cells further suggests that this putative tumor suppressor depends upon AhR to undergo upregulation (Figure 9E). It is likely that AhR, p38, and JNK signaling pathways regulate SF 203-



mediated *CYGB* induction, which results in DNA damage. To the best of our knowledge, this report is the first to evaluate *CYGB* upregulation in breast cancer cells with a potential or established anticancer agent other than an epigenetic agent. Although the most robust induction of *CYGB* occurred in cells exposed to SF 203 for 12 or 24, this induction was evident during brief (3 h) exposures (data not shown). It is therefore plausible that SF 203 upregulates *CYGB* directly, although we cannot rule out the possibility that *CYGB* induction also occurs as a secondary action to activated AhR–CYP–ROS–MAPK signaling.

In summary, we show that the investigational anticancer agent SF 203 increases intracellular ROS that depends, at least partially, on its ability to activate the AhR–CYP pathway. Previous reports demonstrate that SF 203 binds to AhR, which translocates from the cytosol to the nucleus to activate cytochrome P450s 1A1, 1A2, and 1B1.<sup>8,11,44,88</sup> The activation of these genes results in the conversion of SF 203 into metabolites (likely hydroxylamine and/or nitrenium ions) that promote increases in ROS production. Our current study shows that SF 203-mediated increases in ROS culminate in the phosphorylation of stress responsive kinases and that the ensuing DNA damage is likely sustained via a positive feedback loop. The DNA damage then promotes the induction of oxidative stress responsive genes such as putative tumor suppressor *CYGB*. Our findings reveal the amenability of *CYGB* to pharmacological manipulation, and targeting this gene may lead to more effective management of breast cancer and other malignancies.

## AUTHOR INFORMATION

### Corresponding Author

\*Phone: +1 (909) 558-7703; Fax: +1 (909) 558-4035; E-mail: ebrantley@llu.edu.

### Present Address

#(A.D.) MolecularMD, 320 Bent Street, Cambridge, Massachusetts 02141, United States.

### Funding

This work was supported in part by funds from the Departmental of Pharmaceutical and Administrative Sciences (Loma Linda University School of Pharmacy), the Grants to Promote Collaborative and Translational Research Award (Loma Linda University School of Medicine intramural grant), and by the National Institutes of Health (grant nos. RO1GM41336, R01 CA101864-8S, P20MD001632, R25GM082808, and R25GM060507). Petreana Campbell is a recipient of an American Association of University Women International Fellowship.

### Notes

The authors declare no competing financial interest. A portion of this work was presented at the 101st Annual American Association for Cancer Research meeting in Washington, DC, and in partial fulfillment of dissertation requirements (L.S.M.).

## ACKNOWLEDGMENTS

The authors wish to thank Stephanie Cho for her assistance with the comet assay. The authors also thank Dr. Jason Matthews for the AHR100 cells. Additionally, the authors are grateful to Drs. Susan Kane (City of Hope, Duarte, CA) and Penelope Duerksen-Hughes (Loma Linda University, Loma Linda, CA) for their critical evaluation of our manuscript.

## ABBREVIATIONS

ROS; reactive oxygen species; ER; estrogen receptor;  $\alpha$ NF; alpha-naphthoflavone; NAC; N-acetyl-L-cysteine; BAP; benzo[*a*]pyrene; 1,6-BPQ; benzo[*a*]pyrene-1,6-quinone; DOX; doxorubicin; CYGB; cytoglobin; SSBs; single-strand breaks; PTGS2; prostaglandin-endoperoxide synthase 2; KRT1; keratin 1; IPCEF1; interaction protein for cytohesin exchange factors 1; CCS; copper chaperone for superoxide dismutase; GPX2; glutathione peroxidase 2; MSRA; methionine sulfoxide reductase A; AOX1; aldehyde oxidase I; APOE; apolipoprotein E; SRXN1; sulfiredoxin 1 homologue; TPO; thyroid peroxidase; EPHX2; epoxide hydrolase 2 (cytoplasmic)

## REFERENCES

- (1) Ayllon, V., and O'Connor, R. (2007) PBK/TOPK promotes tumour cell proliferation through p38 MAPK activity and regulation of the DNA damage response. *Oncogene* 26, 3451–3461.
- (2) DeSantis, C. E., Lin, C. C., Mariotto, A. B., Siegel, R. L., Stein, K. D., Kramer, J. L., Alteri, R., Robbins, A. S., and Jemal, A. (2014) Cancer treatment and survivorship statistics, 2014. *Ca-Cancer J. Clin.* 64, 252–271.
- (3) DeSantis, C., Ma, J., Bryan, L., and Jemal, A. (2014) Breast cancer statistics, 2013. *Ca-Cancer J. Clin.* 64, 52–62.
- (4) Sastre-Serra, J., Nadal-Serrano, M., Pons, D. G., Valle, A., Garau, I., Garcia-Bonafe, M., Oliver, J., and Roca, P. (2013) The oxidative stress in breast tumors of postmenopausal women is ERalpha/ERbeta ratio dependent. *Free Radical Biol. Med.* 61C, 11–17.
- (5) Behrsing, H. P., Furniss, M. J., Davis, M., Tomaszewski, J. E., and Parchment, R. E. (2013) In vitro exposure of precision-cut lung slices to 2-(4-amino-3-methylphenyl)-5-fluorobenzothiazole lysylamide dihydrochloride (NSC 710305, Phortress) increases inflammatory cytokine content and tissue damage. *Toxicol. Sci.* 131, 470–479.
- (6) Leong, C. O., Gaskell, M., Martin, E. A., Heydon, R. T., Farmer, P. B., Bibby, M. C., Cooper, P. A., Double, J. A., Bradshaw, T. D., and Stevens, M. F. (2003) Antitumor 2-(4-aminophenyl)benzothiazoles generate DNA adducts in sensitive tumour cells in vitro and in vivo. *Br. J. Cancer* 88, 470–477.
- (7) Leong, C. O., Suggett, M., Swaine, D. J., Bibby, M. C., Stevens, M. F., and Bradshaw, T. D. (2004) In vitro, in vivo, and in silico analyses of the antitumor activity of 2-(4-amino-3-methylphenyl)-5-fluorobenzothiazoles. *Mol. Cancer Ther.* 3, 1565–1575.
- (8) Bazzi, R., Bradshaw, T. D., Rowlands, J. C., Stevens, M. F., and Bell, D. R. (2009) 2-(4-Amino-3-methylphenyl)-5-fluorobenzothiazole is a ligand and shows species-specific partial agonism of the aryl hydrocarbon receptor. *Toxicol. Appl. Pharmacol.* 237, 102–110.
- (9) Bradshaw, T. D., Bibby, M. C., Double, J. A., Fichtner, I., Cooper, P. A., Alley, M. C., Donohue, S., Stinson, S. F., Tomaszewski, J. E., Sausville, E. A., and Stevens, M. F. (2002) Preclinical evaluation of amino acid prodrugs of novel antitumor 2-(4-amino-3-methylphenyl)-benzothiazoles. *Mol. Cancer Ther.* 1, 239–246.
- (10) Hose, C. D., Hollingshead, M., Sausville, E. A., and Monks, A. (2003) Induction of CYP1A1 in tumor cells by the antitumor agent 2-[4-amino-3-methylphenyl]-5-fluoro-benzothiazole: a potential surrogate marker for patient sensitivity. *Mol. Cancer Ther.* 2, 1265–1272.
- (11) Trapani, V., Patel, V., Leong, C. O., Ciolino, H. P., Yeh, G. C., Hose, C., Trepel, J. B., Stevens, M. F., Sausville, E. A., and Loaiza-Perez, A. I. (2003) DNA damage and cell cycle arrest induced by 2-(4-amino-3-methylphenyl)-5-fluorobenzothiazole (SF 203, NSC 703786) is attenuated in aryl hydrocarbon receptor deficient MCF-7 cells. *Br. J. Cancer* 88, 599–605.
- (12) Callero, M. A., Luzzani, G. A., De Dios, D. O., Bradshaw, T. D., and Perez, A. I. (2013) Biomarkers of sensitivity to potent and selective antitumor 2-(4-amino-3-methylphenyl)-5-fluorobenzothiazole (SF203) in ovarian cancer. *J. Cell. Biochem.* 114, 2392–2404.
- (13) Reichard, J. F., Dalton, T. P., Shertzer, H. G., and Puga, A. (2005) Induction of oxidative stress responses by dioxin and other ligands of the aryl hydrocarbon receptor. *Dose-Response* 3, 306–331.

- (14) McLean, L., Soto, U., Agama, K., Francis, J., Jimenez, R., Pommier, Y., Sowers, L., and Brantley, E. (2008) Amino flavone induces oxidative DNA damage and reactive oxidative species-mediated apoptosis in breast cancer cells. *Int. J. Cancer* 122, 1665–1674.
- (15) Choi, H., Chun, Y. S., Shin, Y. J., Ye, S. K., Kim, M. S., and Park, J. W. (2008) Curcumin attenuates cytochrome P450 induction in response to 2,3,7,8-tetrachlorodibenzo-*p*-dioxin by ROS-dependently degrading AhR and ARNT. *Cancer Sci.* 99, 2518–2524.
- (16) Nagai, H., Noguchi, T., Takeda, K., and Ichijo, H. (2007) Pathophysiological roles of ASK1–MAP kinase signaling pathways. *J. Biochem. Mol. Biol.* 40, 1–6.
- (17) Matsuzawa, A., and Ichijo, H. (2008) Redox control of cell fate by MAP kinase: physiological roles of ASK1–MAP kinase pathway in stress signaling. *Biochim. Biophys. Acta* 1780, 1325–1336.
- (18) Reddy, K. B., Nabha, S. M., and Atanaskova, N. (2003) Role of MAP kinase in tumor progression and invasion. *Cancer Metastasis Rev.* 22, 395–403.
- (19) Viala, E., and Pouyssegur, J. (2004) Regulation of tumor cell motility by ERK mitogen-activated protein kinases. *Ann. N.Y. Acad. Sci.* 1030, 208–218.
- (20) Cummings, C. T., Deryckere, D., Earp, H. S., and Graham, D. K. (2013) Molecular pathways: MERTK signaling in cancer. *Clin. Cancer Res.* 19, S275–S280.
- (21) Chiu, W. H., Luo, S. J., Chen, C. L., Cheng, J. H., Hsieh, C. Y., Wang, C. Y., Huang, W. C., Su, W. C., and Lin, C. F. (2012) Vinca alkaloids cause aberrant ROS-mediated JNK activation, Mcl-1 downregulation, DNA damage, mitochondrial dysfunction, and apoptosis in lung adenocarcinoma cells. *Biochem. Pharmacol.* 83, 1159–1171.
- (22) Takahashi, S., Ebihara, A., Kajihara, H., Kontani, K., Nishina, H., and Katada, T. (2011) RASSF7 negatively regulates pro-apoptotic JNK signaling by inhibiting the activity of phosphorylated-MKK7. *Cell Death Differ.* 18, 645–655.
- (23) Nikhil, K., Sharan, S., Singh, A. K., Chakraborty, A., and Roy, P. (2014) Anticancer activities of pterostilbene–isothiocyanate conjugate in breast cancer cells: involvement of PPARgamma. *PLoS One* 9, e104592.
- (24) Le, X. F., Varela, C. R., and Bast, R. C., Jr. (2002) Heregulin-induced apoptosis. *Apoptosis* 7, 483–491.
- (25) Song, G. Q., and Zhao, Y. (2013) Different therapeutic effects of distinct KISS1 fragments on breast cancer in vitro and in vivo. *Int. J. Oncol.* 43, 1219–1227.
- (26) Biswas, N., Mahato, S. K., Chowdhury, A. A., Chaudhuri, J., Manna, A., Vinayagam, J., Chatterjee, S., Jaisankar, P., Chaudhuri, U., and Bandyopadhyay, S. (2012) ICB3E induces iNOS expression by ROS-dependent JNK and ERK activation for apoptosis of leukemic cells. *Apoptosis* 17, 612–626.
- (27) Yang, T. Y., Chang, G. C., Chen, K. C., Hung, H. W., Hsu, K. H., Sheu, G. T., and Hsu, S. L. (2011) Sustained activation of ERK and Cdk2/cyclin-A signaling pathway by pemetrexed leading to S-phase arrest and apoptosis in human non-small cell lung cancer A549 cells. *Eur. J. Pharmacol.* 663, 17–26.
- (28) Li, X., Wang, K., Ren, Y., Zhang, L., Tang, X. J., Zhang, H. M., Zhao, C. Q., Liu, P. J., Zhang, J. M., and He, J. J. (2014) MAPK signaling mediates sinomenine hydrochloride-induced human breast cancer cell death via both reactive oxygen species-dependent and -independent pathways: an in vitro and in vivo study. *Cell Death Dis.* 5, e1356.
- (29) Tan, Z., Chang, X., Puga, A., and Xia, Y. (2002) Activation of mitogen-activated protein kinases (MAPKs) by aromatic hydrocarbons: role in the regulation of aryl hydrocarbon receptor (AHR) function. *Biochem. Pharmacol.* 64, 771–780.
- (30) Weiss, C., Faust, D., Durk, H., Kolluri, S. K., Pelzer, A., Schneider, S., Dietrich, C., Oesch, F., and Gottlicher, M. (2005) TCDD induces c-jun expression via a novel Ah (dioxin) receptor-mediated p38-MAPK-dependent pathway. *Oncogene* 24, 4975–4983.
- (31) Xiang, T., Li, L., Yin, X., Zhong, L., Peng, W., Qiu, Z., Ren, G., and Tao, Q. (2013) Epigenetic silencing of the WNT antagonist Dickkopf 3 disrupts normal Wnt/beta-catenin signalling and apoptosis regulation in breast cancer cells. *J. Cell Mol. Med.* 17, 1236–1246.
- (32) Tront, J. S., Huang, Y., Fornace, A. J., Jr., Hoffman, B., and Liebermann, D. A. (2010) Gadd45a functions as a promoter or suppressor of breast cancer dependent on the oncogenic stress. *Cancer Res.* 70, 9671–9681.
- (33) Tront, J. S., Hoffman, B., and Liebermann, D. A. (2006) Gadd45a suppresses Ras-driven mammary tumorigenesis by activation of c-Jun NH2-terminal kinase and p38 stress signaling resulting in apoptosis and senescence. *Cancer Res.* 66, 8448–8454.
- (34) Cazillis, M., Bringuier, A. F., Delautier, D., Buisine, M., Bernuau, D., Gespach, C., and Groyer, A. (2004) Disruption of MKK4 signaling reveals its tumor-suppressor role in embryonic stem cells. *Oncogene* 23, 4735–4744.
- (35) Brantley, E., Antony, S., Kohlhagen, G., Meng, L., Agama, K., Stinson, S. F., Sausville, E. A., and Pommier, Y. (2006) Anti-tumor drug candidate 2-(4-amino-3-methylphenyl)-5-fluorobenzothiazole induces single-strand breaks and DNA–protein cross-links in sensitive MCF-7 breast cancer cells. *Cancer Chemother. Pharmacol.* 58, 62–72.
- (36) Yeh, G. C., Daschner, P. J., Lopaczynska, J., MacDonald, C. J., and Ciolino, H. P. (2001) Modulation of glucose-6-phosphate dehydrogenase activity and expression is associated with aryl hydrocarbon resistance in vitro. *J. Biol. Chem.* 276, 34708–34713.
- (37) Celius, T., and Matthews, J. (2010) Functional analysis of six human aryl hydrocarbon receptor variants in human breast cancer and mouse hepatoma cell lines. *Toxicology* 277, 59–65.
- (38) Coccolakis, E., Lemay, S., Ali, S., and Lebrun, J. J. (2001) The p38 MAPK pathway is required for cell growth inhibition of human breast cancer cells in response to activin. *J. Biol. Chem.* 276, 18430–18436.
- (39) GraphPad Prism, 4.0, Graph Pad Software, Inc., San Diego, CA, www.graphpad.com.
- (40) Burdick, A. D., Davis, J. W., II, Liu, K. J., Hudson, L. G., Shi, H., Monske, M. L., and Burchiel, S. W. (2003) Benzo(a)pyrene quinones increase cell proliferation, generate reactive oxygen species, and transactivate the epidermal growth factor receptor in breast epithelial cells. *Cancer Res.* 63, 7825–7833.
- (41) Shigenaga, M. K., Aboujaoude, E. N., Chen, Q., and Ames, B. N. (1994) Assays of oxidative DNA damage biomarkers 8-oxo-2'-deoxyguanosine and 8-oxoguanine in nuclear DNA and biological fluids by high-performance liquid chromatography with electrochemical detection. *Methods Enzymol.* 234, 16–33.
- (42) Babbar, N., and Casero, R. A., Jr. (2006) Tumor necrosis factor- $\alpha$  increases reactive oxygen species by inducing spermine oxidase in human lung epithelial cells: a potential mechanism for inflammation-induced carcinogenesis. *Cancer Res.* 66, 11125–11130.
- (43) Carmody, R. J., and Cotter, T. G. (2001) Signalling apoptosis: a radical approach. *Redox Rep.* 6, 77–90.
- (44) Brantley, E., Trapani, V., Alley, M. C., Hose, C. D., Bradshaw, T. D., Stevens, M. F., Sausville, E. A., and Stinson, S. F. (2004) Fluorinated 2-(4-amino-3-methylphenyl)benzothiazoles induce CYP1A1 expression, become metabolized, and bind to macromolecules in sensitive human cancer cells. *Drug Metab. Dispos.* 32, 1392–1401.
- (45) Zangar, R. C., Davydov, D. R., and Verma, S. (2004) Mechanisms that regulate production of reactive oxygen species by cytochrome P450. *Toxicol. Appl. Pharmacol.* 199, 316–331.
- (46) Deng, Y. T., Huang, H. C., and Lin, J. K. (2010) Rotenone induces apoptosis in MCF-7 human breast cancer cell-mediated ROS through JNK and p38 signaling. *Mol. Carcinog.* 49, 141–151.
- (47) Xiao, D., Powolny, A. A., and Singh, S. V. (2008) Benzyl isothiocyanate targets mitochondrial respiratory chain to trigger reactive oxygen species-dependent apoptosis in human breast cancer cells. *J. Biol. Chem.* 283, 30151–30163.
- (48) Liu, B., Cheng, Y., Bian, H. J., and Bao, J. K. (2009) Molecular mechanisms of *Polygonatum cyrtoneuma* lectin-induced apoptosis and autophagy in cancer cells. *Autophagy* 5, 253–255.
- (49) Li, L., Abdel Fattah, E., Cao, G., Ren, C., Yang, G., Goltsov, A. A., Chinault, A. C., Cai, W. W., Timme, T. L., and Thompson, T. C.

- (2008) Glioma pathogenesis-related protein 1 exerts tumor suppressor activities through proapoptotic reactive oxygen species-c-Jun-NH<sub>2</sub> kinase signaling. *Cancer Res.* 68, 434–443.
- (50) Wei, X., Guo, W., Wu, S., Wang, L., Huang, P., Liu, J., and Fang, B. (2010) Oxidative stress in NSC-741909-induced apoptosis of cancer cells. *J. Transl. Med.* 8, 37.
- (51) Kuo, P. L., Chen, C. Y., Tzeng, T. F., Lin, C. C., and Hsu, Y. L. (2010) Involvement of reactive oxygen species/c-Jun NH<sub>2</sub>-terminal kinase pathway in kotomolide A induces apoptosis in human breast cancer cells. *Toxicol. Appl. Pharmacol.* 229, 215–226.
- (52) Hong, E. H., Lee, S. J., Kim, J. S., Lee, K. H., Um, H. D., Kim, J. H., Kim, S. J., Kim, J. I., and Hwang, S. G. (2010) Ionizing radiation induces cellular senescence of articular chondrocytes via negative regulation of SIRT1 by p38 kinase. *J. Biol. Chem.* 285, 1283–1295.
- (53) Yue, P., Zhou, Z., Khuri, F. R., and Sun, S. Y. (2006) Depletion of intracellular glutathione contributes to JNK-mediated death receptor 5 upregulation and apoptosis induction by the novel synthetic triterpenoid methyl-2-cyano-3,12-dioxooleana-1,9-dien-28-oate (CDDO-Me). *Cancer Biol. Ther.* 5, 492–497.
- (54) Moore, R. J., Chamberlain, R. M., and Khuri, F. R. (2004) Apolipoprotein E and the risk of breast cancer in African-American and non-Hispanic white women. A review. *Oncology* 66, 79–93.
- (55) Brigelius-Flohe, R., and Kipp, A. (2009) Glutathione peroxidases in different stages of carcinogenesis. *Biochim. Biophys. Acta* 1790, 1555–1568.
- (56) White, D. T., McShea, K. M., Attar, M. A., and Santy, L. C. (2010) GRASP and IPCEF promote ARF-to-Rac signaling and cell migration by coordinating the association of ARNO/cytohesin 2 with Dock180. *Mol. Biol. Cell* 21, 562–571.
- (57) Shivapurkar, N., Stastny, V., Okumura, N., Girard, L., Xie, Y., Prinsen, C., Thunnissen, F. B., Wistuba, I. I., Czerniak, B., Frenkel, E., Roth, J. A., Liloglou, T., Xinarianos, G., Field, J. K., Minna, J. D., and Gazdar, A. F. (2008) Cytochrome, the newest member of the globin family, functions as a tumor suppressor gene. *Cancer Res.* 68, 7448–7456.
- (58) Mammen, P. P., Shelton, J. M., Ye, Q., Kanatous, S. B., McGrath, A. J., Richardson, J. A., and Garry, D. J. (2006) Cytochrome is a stress-responsive hemoprotein expressed in the developing and adult brain. *J. Histochem. Cytochem.* 54, 1349–1361.
- (59) Sun, Y. W., Herzog, C. R., Krzeminski, J., Amin, S., Perdew, G., and El-Bayoumy, K. (2007) Effects of the environmental mammary carcinogen 6-nitrochrysene on p53 and p21<sup>Cip1</sup> protein expression and cell cycle regulation in MCF-7 and MCF-10A cells. *Chem.-Biol. Interact.* 170, 31–39.
- (60) Singletary, K., and MacDonald, C. (2000) Inhibition of benzo[a]pyrene- and 1,6-dinitropyrene-DNA adduct formation in human mammary epithelial cells by dibenzoylmethane and sulforaphane. *Cancer Lett.* 155, 47–54.
- (61) Hutchinson, I., Chua, M. S., Browne, H. L., Trapani, V., Bradshaw, T. D., Westwell, A. D., and Stevens, M. F. (2001) Antitumor benzothiazoles. 14. Synthesis and in vitro biological properties of fluorinated 2-(4-aminophenyl)benzothiazoles. *J. Med. Chem.* 44, 1446–1455.
- (62) Wang, K., and Guengerich, F. P. (2012) Bioactivation of fluorinated 2-aryl-benzothiazole antitumor molecules by human cytochrome P450s 1A1 and 2W1 and deactivation by cytochrome P450 2S1. *Chem. Res. Toxicol.* 25, 1740–1751.
- (63) Bradshaw, T. D., Stone, E. L., Trapani, V., Leong, C. O., Matthews, C. S., te Poele, R., and Stevens, M. F. (2008) Mechanisms of acquired resistance to 2-(4-amino-3-methylphenyl)benzothiazole in breast cancer cell lines. *Breast Cancer Res. Treat.* 110, 57–68.
- (64) Matsukawa, J., Matsuzawa, A., Takeda, K., and Ichijo, H. (2004) The ASK1-MAP kinase cascades in mammalian stress response. *J. Biochem.* 136, 261–265.
- (65) Brozovic, A., and Osmak, M. (2007) Activation of mitogen-activated protein kinases by cisplatin and their role in cisplatin-resistance. *Cancer Lett.* 251, 1–16.
- (66) Ghose, R., Omolubi, O., Gandhi, A., Shah, P., Strohacker, K., Carpenter, K. C., McFarlin, B., and Guo, T. (2011) Role of high-fat diet in regulation of gene expression of drug metabolizing enzymes and transporters. *Life Sci.* 89, 57–64.
- (67) Fan, S., Qi, M., Yu, Y., Li, L., Yao, G., Tashiro, S., Onodera, S., and Ikejima, T. (2012) p53 activation plays a crucial role in silibinin induced ROS generation via PUMA and JNK. *Free Radical Res.* 46, 310–319.
- (68) Qi, M., Zhou, H., Fan, S., Li, Z., Yao, G., Tashiro, S., Onodera, S., Xia, M., and Ikejima, T. (2013) mTOR inactivation by ROS-JNK-p53 pathway plays an essential role in p53-induced acid B induced autophagy-dependent senescence in murine fibrosarcoma L929 cells. *Eur. J. Pharmacol.* 715, 76–88.
- (69) Shi, Y., Nikulnikov, F., Zawacka-Pankau, J., Li, H., Gabdoulina, R., Xu, J., Eriksson, S., Hedstrom, E., Issaeva, N., Kel, A., Arner, E. S., and Selivanova, G. (2014) ROS-dependent activation of JNK converts p53 into an efficient inhibitor of oncogenes leading to robust apoptosis. *Cell Death Differ.* 21, 612–623.
- (70) Palanivel, K., Kanimozhi, V., Kadalmani, B., and Akbarsha, M. A. (2014) Verrucarin A induces apoptosis through ROS-mediated EGFR/MAPK/Akt signaling pathways in MDA-MB-231 breast cancer cells. *J. Cell. Biochem.* 115, 2022–2032.
- (71) Mandlekar, S., and Kong, A. N. (2001) Mechanisms of tamoxifen-induced apoptosis. *Apoptosis* 6, 469–477.
- (72) Miao, W., Hu, L., Scrivens, P. J., and Batist, G. (2005) Transcriptional regulation of NF-E2 p45-related factor (NRF2) expression by the aryl hydrocarbon receptor-xenobiotic response element signaling pathway: direct cross-talk between phase I and II drug-metabolizing enzymes. *J. Biol. Chem.* 280, 20340–20348.
- (73) Okino, S. T., Pookot, D., Basak, S., and Dahiya, R. (2009) Toxic and chemopreventive ligands preferentially activate distinct aryl hydrocarbon receptor pathways: implications for cancer prevention. *Cancer Prev. Res.* 2, 251–256.
- (74) Hestermann, E. V., and Brown, M. (2003) Agonist and chemopreventive ligands induce differential transcriptional cofactor recruitment by aryl hydrocarbon receptor. *Mol. Cell. Biol.* 23, 7920–7925.
- (75) Safe, S., Qin, C., and McDougal, A. (1999) Development of selective aryl hydrocarbon receptor modulators for treatment of breast cancer. *Expert Opin. Invest. Drugs* 8, 1385–1396.
- (76) Ramamoorthy, K., Gupta, M. S., Sun, G., McDougal, A., and Safe, S. H. (1999) 3,3',4,4'-Tetrachlorobiphenyl exhibits antiestrogenic and antitumorigenic activity in the rodent uterus and mammary cells and in human breast cancer cells. *Carcinogenesis* 20, 115–123.
- (77) Hall, J. M., Barhoover, M. A., Kazmin, D., McDonnell, D. P., Greenlee, W. F., and Thomas, R. S. (2010) Activation of the aryl-hydrocarbon receptor inhibits invasive and metastatic features of human breast cancer cells and promotes breast cancer cell differentiation. *Mol. Endocrinol.* 24, 359–369.
- (78) Wormke, M., Stoner, M., Saville, B., Walker, K., Abdelrahim, M., Burghardt, R., and Safe, S. (2003) The aryl hydrocarbon receptor mediates degradation of estrogen receptor alpha through activation of proteasomes. *Mol. Cell. Biol.* 23, 1843–1855.
- (79) Ohtake, F., Baba, A., Takada, I., Okada, M., Iwasaki, K., Miki, H., Takahashi, S., Kouzmenko, A., Nohara, K., Chiba, T., Fujii-Kuriyama, Y., and Kato, S. (2007) Dioxin receptor is a ligand-dependent E3 ubiquitin ligase. *Nature* 446, 562–566.
- (80) Zhang, S., Lei, P., Liu, X., Li, X., Walker, K., Kotha, L., Rowlands, C., and Safe, S. (2009) The aryl hydrocarbon receptor as a target for estrogen receptor-negative breast cancer chemotherapy. *Endocr.-Relat. Cancer* 16, 835–844.
- (81) Meng, L. H., Shankavaram, U., Chen, C., Agama, K., Fu, H. Q., Gonzalez, F. J., Weinstein, J., and Pommier, Y. (2006) Activation of aminoflavone (NSC 686288) by a sulfotransferase is required for the antiproliferative effect of the drug and for induction of histone gamma-H2AX. *Cancer Res.* 66, 9656–9664.
- (82) Stark, K., Burger, A., Wu, J., Shelton, P., Polin, L., and Li, J. (2013) Reactivation of estrogen receptor alpha by vorinostat sensitizes mesenchymal-like triple-negative breast cancer to aminoflavone, a ligand of the aryl hydrocarbon receptor. *PLoS One* 8, e74525.



(83) Mimura, I., Nangaku, M., Nishi, H., Inagi, R., Tanaka, T., and Fujita, T. (2010) Cytoglobin, a novel globin, plays an antifibrotic role in the kidney. *Am. J. Physiol.: Renal Physiol.* 299, F1120–F1133.

(84) Nishi, H., Inagi, R., Kawada, N., Yoshizato, K., Mimura, I., Fujita, T., and Nangaku, M. (2011) Cytoglobin, a novel member of the globin family, protects kidney fibroblasts against oxidative stress under ischemic conditions. *Am. J. Pathol.* 178, 128–139.

(85) Oleksiewicz, U., Liloglou, T., Tasopoulou, K. M., Daskoulidou, N., Bryan, J., Gosney, J. R., Field, J. K., and Xinarianos, G. (2013) Cytoglobin has bimodal: tumour suppressor and oncogene functions in lung cancer cell lines. *Hum. Mol. Genet.* 22, 3207–3217.

(86) Kovacic, P., and Somanathan, R. (2011) Recent developments in the mechanism of anticancer agents based on electron transfer, reactive oxygen species and oxidative stress. *Anti-Cancer Agents Med. Chem.* 11, 658–668.

(87) Kovacic, H., and Somanathan, R. (2011) Novel, unifying mechanism for aromatic primary-amines (therapeutics, carcinogens and toxins): electron transfer, reactive oxygen species, oxidative stress and metabolites. *MedChemComm* 2, 106–112.

(88) Bradshaw, T. D., and Westwell, A. D. (2004) The development of the antitumour benzothiazole prodrug, Phortress, as a clinical candidate. *Curr. Med. Chem.* 11, 1009–1021.